

# PHOTOPHYSICAL ANALYSIS OF 2,3-DIPHENYL FUMARONITRILE AND PHENOTHIAZINE DYADS

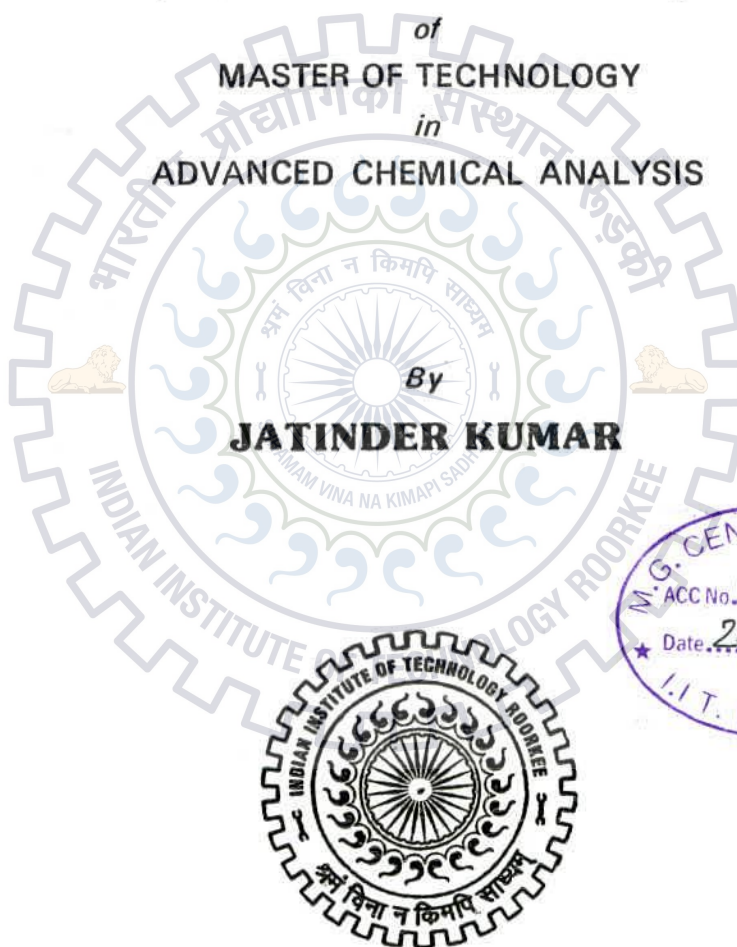
## A DISSERTATION

*Submitted in partial fulfillment of the  
requirements for the award of the degree*

of  
MASTER OF TECHNOLOGY  
in  
ADVANCED CHEMICAL ANALYSIS

By

**JATINDER KUMAR**



DEPARTMENT OF CHEMISTRY  
INDIAN INSTITUTE OF TECHNOLOGY ROORKEE  
ROORKEE - 247 667 (INDIA)  
JUNE, 2013

## **CANDIDATE'S DECLARATION**

I hereby, declare that the work which is being presented in this dissertation entitled **“PHOTOPHYSICAL ANALYSIS OF 2,3-DIPHENYL FUMARONITRILE AND PHENOTHIAZINE DYADS”** in partial fulfillment of the requirements for the award of the degree of **Master of Technology** in **“Advanced Chemical Analysis”** and submitted in the **Department of Chemistry** at **Indian Institute of Technology Roorkee**, is an authentic record of the work carried out by me during the period August 2012 to May 2013, under the guidance of **Dr. K. R. Justin Thomas**, Associate Professor, Department of Chemistry, Indian Institute of Technology Roorkee, Roorkee.

The matter presented in this dissertation work has not been submitted by me for the award of any degree of this or any other institute/ University. In keeping with the general practice of reporting scientific observation, due acknowledgement has been made wherever the work described is based on the findings of other investigators.

Date: 24<sup>th</sup> May, 2013

Place: Roorkee

  
(Jatinder Kumar)

## **CERTIFICATE**

This is to certify that the above statement made by the candidate is correct to the best of my knowledge.

  
(Dr. K. R. Justin Thomas)

Associate Professor

Department of Chemistry

Indian Institute of Technology Roorkee

ROORKEE-247667 (INDIA)

## **Acknowledgement**

During my research work I received a lot of cooperation, support and encouragement with my supervisor, colleagues and friends. It could be possible for me to finish my dissertation work with their dedication, prayers, wishes, blessings and support.

It is my great pleasure to thank God and the other people who helped me directly or indirectly in the course of my entire journey towards producing this thesis. First and foremost, I must thank my supervisor **Dr. K. R. Justin Thomas**, who helped me a lot in each and every step of my research work. Without his innovative guidance and encouragement, it would be impossible to bring my research work to completion. He always encouraged and enlightened me through his knowledge, intelligence and experience. He trained my scientific skills and aptitude to face every situation during my research and academic carrier that will be obliging for me in my future. He is, and always will be the inspiration to me throughout my life.

I would like to thank all the faculty members of the Chemistry Department for their invaluable help and suggestions during my research. I express my sincere thanks to Mr. Abdul Hauq, in-charge of instrumentation, Department of Chemistry for helping me a lot in carrying out UV-Visible spectroscopy, Fourier transform infrared spectroscopy (FT-IR), and fluorescence measurements. I am also thankful to Mr. Madan Pal, Department of Chemistry, for their technical help during my presentations in the department. I am also thankful to Institute Instrumentation Centre, IIT Roorkee to availed the NMR and TGA facility..

I would like to express my sincere and special thanks to Govardhan Babu for assistance in synthesis. Also I am grateful thanks to my other lab mates for their co-operation support and help in all the ways throughout my research work. They always motivated and encouraged me in my tough times, gave me moral support whenever I felt alone.

Finally, I am highly grateful to my family members specially my father, Shri Ram Adhar and my mother Mrs. Sheela Devi for being the main inspiration and motivating source in this endeavor.

Finally, I must thank all those whom I have failed to state here but have helped in various ways during the course of my research.

**(JATINDER KUMAR)**

# Table of Contents

	Candidate's declaration	i
	Acknowledgements	ii
Chapter 1	<b>Fumaronitrile and phenothiazene based functional materials :</b>	
	<b>A brief survey</b>	
1.1	Introduction	1
1.2	Fumaronitrile based functionalized organic materials	3
1.3	Acrylonitrile based functionalized organic materials	14
1.4	Phenothiazine containing organic materials	14
1.5	Aim and scope	19
Chapter 2	<b>Synthesis and characterization of 2, 3-diphenyl fumaronitrile and phenothiazine dyads</b>	
2.1	Materials and methods	20
2.2	Synthesis of compounds	21
Chapter 3	<b>Photophysical analysis of 2,3-diphenyl fumaronitrile and phenothiazine dyads</b>	
3.1	Introduction	27
3.2	Photophysical properties	28
3.3	Conclusions	41
Chapter 4	Summary	42
	References	44
	Supporting information	49

# Fumaronitrile and phenothiazine based functional materials: A brief survey

## 1.1 Introduction

Organic materials exhibit good photoluminescent responses and attracted considerable interest due to their potential application in electronics and optoelectronics.  $\pi$ -Conjugated organic system with donor-acceptor (D-A) moiety showing a wide range of interesting optical, electrical, and photovoltaic properties in the solid state.<sup>1</sup> Among their many application fields, electroluminescence (EL) devices using small molar mass organic materials have become the most popular technology that have already been employed in practical applications such as flexible devices. Organic materials have advantages over inorganic ones such as low cost, environmental friendly and the ease of handling. In addition to that, linkage of functional groups and enlargement in molecule has endowed the molecular structural properties, lead to interesting and unique electrical and photovoltaic properties.<sup>2-4</sup> Also providing light weight flexible structure for eco friendly and low cost manufacturing processes such as ink-jet printing.<sup>5-9</sup> In the dilute solutions, most of the  $\pi$ -conjugated organic compounds are highly emissive in nature but when they are fabricated into devices become weakly luminescent.<sup>10</sup> Organic molecules in their solid state aggregates to form excimers as less emissive species, which reduces the luminescence efficiency in the devices.<sup>11</sup> Most of the conjugated organic compounds as a promising materials are utilized in the form of thin solid films in their application. Many research groups have attempted or even doing laboratory experiments to diminish or reduce molecular aggregation

(excimers formation) through engineering approaches and physical and chemical modifications in the organic system. Swager et al. in their research, they found higher quantum yield (3.5 times more) of fluorescence ( $\Phi_F$ ) for poly(p-phenylenethylene) film than solution state.<sup>12-13</sup> Important features of organic materials are stability and their emission in the solid state & on fabrication used as organic light-emitting diodes (OLEDs)<sup>14</sup> Conjugated organic compounds usually in solution state exhibit weak emission than in solid state. In solid state significant and prominent emission is due to electron transfer and intermolecular energy transfer.<sup>15</sup> Therefore, main objective in the research is to prepare organic materials with high emissive efficiency. D-A compounds containing aromatic fumaronitrile core (as strong acceptor) have significant attention as novel promising candidates in EL devices because of their strong emission in the solid state.<sup>16,17</sup>

An electroluminescent (EL) device is a multilayered component device mainly comprises a light emitting layer, an electron transporting layer, as well as a hole transporting layer. Therefore, the EL performance significantly depends upon the recombination efficiency of the holes and electrons injected from the anode and cathode respectively. By optimizing the charge flux balance, improve the device efficiency and limiting of the light consumption because the hole-transporting materials has a higher carrier drift than the electron transporting materials in most organic light emitting diodes (OLEDs) materials. Bipolar materials with emission characteristics incorporating both electron- and hole- transporting segments can effectively stabilize exciton formation and balance the hole and electron charge in the emitting layer.<sup>18-21</sup> Bipolar compounds has significantly structured the device with double layers or even a single layer, which will limit the overall cost and accelerate its ongoing commercialization activities. Similarly, dye-sensitized solar cell (DSSC) system based on the highly porous nanocrystalline TiO<sub>2</sub> films which are

technologically considerable due to their demonstrated high power conversion efficiency, low cost and highly semiconductor stability. In DSSCs sensitizer is a critical component.<sup>22,23</sup> Both organometallic and organic sensitizers are promising candidates for application in DSSCs. But organic dyes have some advantages over organometallic complexes such as eco friendly, highly flexibility in their structure, low cost, easier in manufacturing and purification, show large spectral response in wider solar system etc. Organic dyes featured with donor-acceptor molecular configuration which favors charge separation within molecule and provides high rates of collection of electrons at terminal electrode.

Since, the dissertation is concerned about synthesis of 2,3-diphenyl fumaronitrile and phenothiazine dyads for application in optoelectronic devices, herein, we briefly commence on the usefulness of the molecular organic materials based on 2,3-diphenyl fumaronitrile and phenothiazine.

## **1.2 Fumaronitrile based functionalized organic materials**

Fumaronitrile is a well known compound having strong acceptor ability due to presence of two electron withdrawing cyanide groups in conjugation. D-A compounds with aromatic fumaronitrile core shows significant features of promising candidate for the EL devices with high emission efficiency in the solid state.<sup>24-26</sup> There is a assumption and hypothetical approach behind the enhanced emission by organic materials in the solid state is due to intermolecular interaction and specific type of aggregation (H- or J-aggregation) in such conjugated organic materials. Such type of aggregation in organic materials produces enhanced emission, so as enhanced emissive materials becomes a promising candidate for OLEDs application as highly efficient emitters.<sup>13,27</sup> Fumaronitrile core based conjugated organic compounds shows not only intense luminescence in both solution and solid state but also shows excellent stability. To

achieve the stable efficient organic materials for electronic and optoelectronics applications, it is important to achieve correlation between fluorescence quantum yield ( $\Phi_F$ ) and conjugation effect in the organic system.<sup>28</sup> Therefore, herein we also tried to find the direct correlation in between conjugation, functional groups, donor-acceptor potency and fluorescence quantum yield ( $\Phi_F$ ). Organic system containing diphenyl fumaronitrile moiety as strong acceptor core, reduced fluorescence quenching in the solid state because of anti-parallel dipole interactions.<sup>29</sup>

We present below some of reported fumaronitrile core based functionalized organic materials for OLEDs, DSSCs and bioimaging application. For example, donor-linker-acceptor (D- $\pi$ -A), donor-linker-acceptor-linker-donor (D- $\pi$ -A- $\pi$ -D) system with aromatic fumaronitrile core in which fumaronitrile core act as strong acceptor and indole, phenylindole substituents act as donor. In the photophysical analysis, these molecules showed intense absorption band in blue- to green region and intense emission band in blue- to red region. Shifting in the absorption and emission band was due to  $\pi$ -linker, electron donor moieties and solvents properties. Quantum yields ( $\Phi_F$ ) of these compounds were moderate in solution state rather higher in the solid state.<sup>30</sup>

Kinstel et al.<sup>30</sup> reported a novel series of organic compounds (**F1-F5**) containing aromatic fumaronitrile core shown in Figure 1. 2,3-bis(4-(1*H*-indol-1-yl)phenyl) fumaronitrile (**F1**), 2,3-bis(4-(2-phenyl-1*H*-indol-1-yl) phenyl) fumaronitrile (**F2**), 2,3-bis(4-(diphenylamino)phenyl) fumaronitrile(**F3**), 2,3-bis(4-(2-(4-(diphenylamino)phenyl) ethyl)phenyl) fumaronitrile (**F4**), and 2,3-bis(4-(2-(4-(3,6-ditert-butyl-9*H*-carbazol-9-yl)phenyl) ethyl)phenyl) fumaronitrile (**F5**). Color of compounds **F1-F5**, are yellow, deep orange, red, dark red, and orange, respectively. This series of compounds are very much stable in solid state and all are soluble in common organic solvents like toluene, DCM, THF and ACN. These compounds showed enhanced emission solvatochromic which is due to change in the solvents, lead to a large shift in emission



maxima and successive decrease in fluorescence intensity. Fluorescence life time vary from <1 to 7 ns in different solvents.

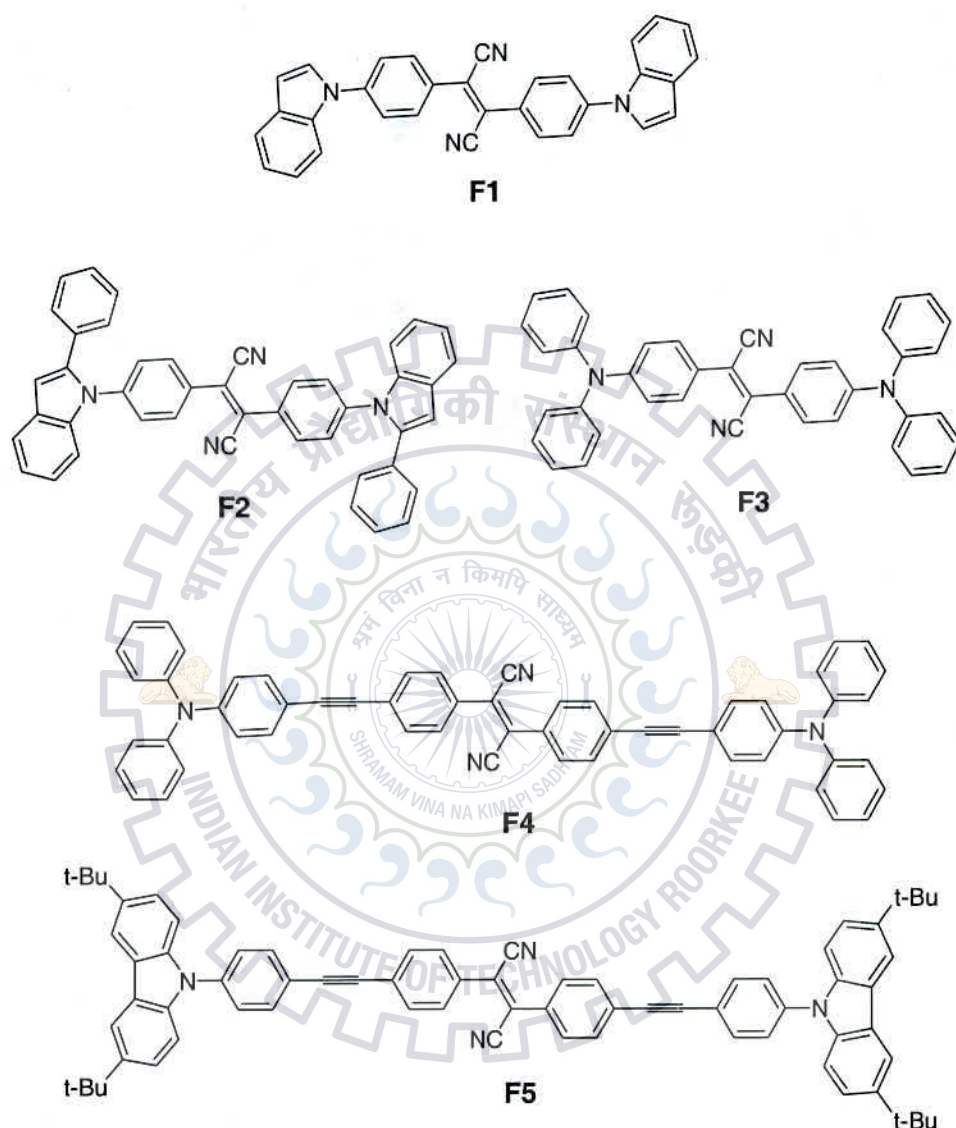


**Figure 1.** Structures of the compounds **F1- F5**

They successfully attained correlation of the properties of functional groups, linkers with optical properties in some extent. From all analysis of these compounds makes them be a promising functionalize materials as colorimetric and pH sensors which were demonstrated with

observable changes in color and luminescence on addition of trifluoroacetic acid. So as these compounds has potential ability for electronic and optoelectronic devices.

Douglas C. Neckers et al.<sup>31</sup> synthesized donor-acceptor compounds (**F6-F7**) (Figure 2) with carbazole as donor moiety and diphenyl fumaronitrile as strong acceptor. 1,2-dicyano-trans-1,2-bis-4-(carbazolyl)phenylethylene (**F6**) and 1,2-dicyano-trans-1,2-bis-4-(3,6-ditert-butylcarbazolyl) phenylethylene (**F7**).

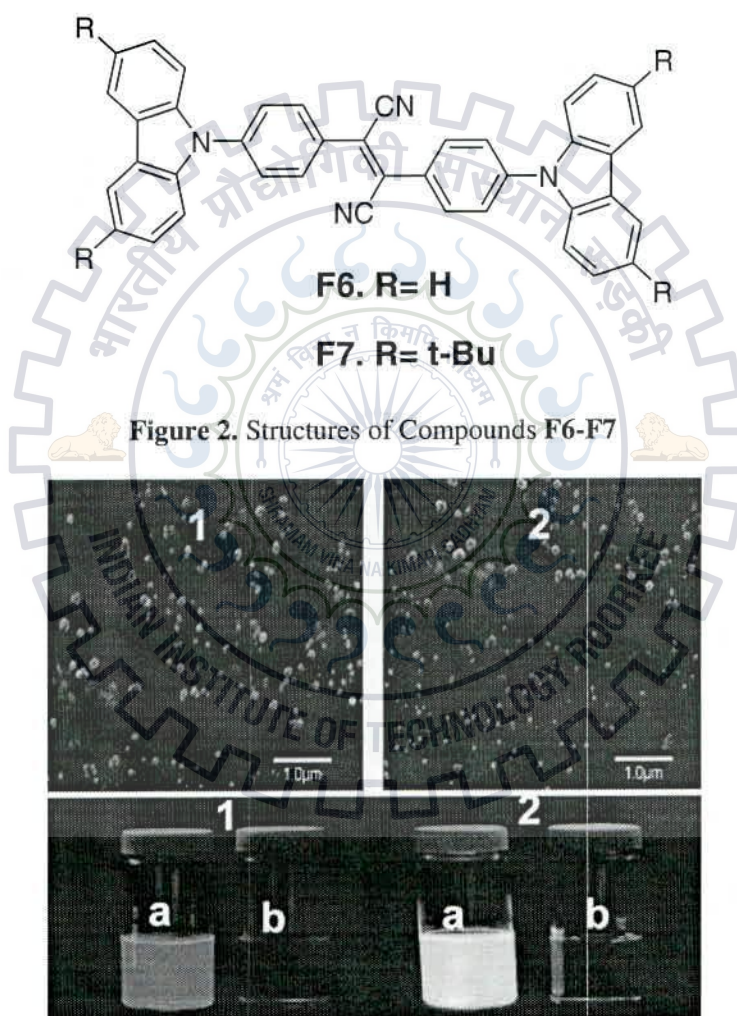


**Figure 3.**

**Figure 3.** Top- SEM images of **F6** (1) and **F7** (2) NPs in water/THF (9:1) mixture, Bottom- Pictures of **F6** (1) and **F7** (2) taken in water/THF (9:1) mixture (a) and in THF (b) under UV light (365nm). Concentration of compound **F6** and **F7** =  $1 \times 10^{-5}$  mol L<sup>-1</sup>

In photophysical analysis, (Table 1) these compounds showed negative solvatochromism in absorption, but in fluorescence exhibited both negative as well positive solvatochromism. These compounds formed 50-150 nm sized nanoparticles as fluorescent organic particles (FOPs) on aggregation in water/THF mixture (Figure 3). FOPs comparatively showed more emission than untreated compound **F6** and **F7**

**Table 1.** Photophysical properties of **F6** and **F7**<sup>a</sup>

Solvents	$\lambda_{max}$	$\lambda_{max}$ (nm)	$\Phi_F$
<b>Compound F6</b>			
CCl <sub>4</sub>	445	530	0.37
DCM	435	618	0.07
THF	423	608	0.02
DMF	415	520	<0.01
Thin film	455	608	0.72
NPs	453	590	0.70
<b>Compound F7</b>			
CCl <sub>4</sub>	470	568	0.44
DCM	457	670	0.01
THF	446	638	<0.01
DMF	440	518	<0.01
Thin film	478	533	0.88
NPs	472	550	0.81

<sup>a</sup>  $\Phi_F$  calculated in solution with riboflavin (0.30 in ethanol) as a reference.  $\Phi_F$  calculated in solid state measured by using integrating sphere.

Wang Y. et al.<sup>32</sup> prepared three red fluorescent dyes **F8-F10** (Figure 4) which are based on arylamino fumaronitrile derivatives as bis(4-(N-(1-naphthyl)phenylamino)-phenyl) fumaronitrile (NPAFN, **F8**), bis(4-(N-(2-naphthyl)phenylamino)phenyl) fumaronitrile (NPAFN, **F9**), and bis(4-(N-(9,9-diethyl-2-fluorenyl)phenylamino)phenyl) fumaronitrile (EFPAFN, **F10**). These dyes showed highly red photoluminescence upon excitation at 635, 650, 658nm for **F8**, **F9** & **F10** respectively. These dyes used as red emitters in multilayered non-doped electroluminescent devices fabrication.

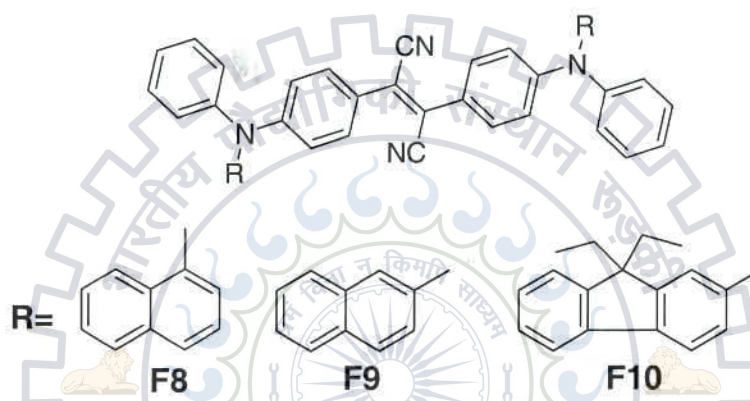


**Figure 4.** Structures of red fluorescent dyes (**F8-F10**)

Tang B.Z. et al.<sup>33</sup> new fumaronitrile-based fluorogen, 2-(4-bromophenyl)-3-(4'-(dimethylamino)-biphenyl-4-yl) fumaronitrile (BDABFN, **F11**) was synthesized which showed aggregation induced emission. This fluorogen incorporated with *N,N*-dimethyl (as donor group) biphenyl fumaronitrile (as acceptor group), and showed an aggregation induced emission (AIE) property. Target fluorogen (BDABFN) structure is mentioned in the Figure 5. This fluorogen showed strong emission (in red-to near IR region) at 653 and 710 nm in its amorphous and cryatalline state respectively.  $\Phi_F$  (fluorescence quantum efficiency) of BDABFN was very high (26.5%) in the solid state. In crystallographic analysis, found that there was no  $\pi$ - $\pi$  stacking and aggregation (*J*- or *H*- aggregation) in the molecule. Unique type of solvatochromism observed in

in the fluorogen due to the presence of strong donor-acceptor intramolecular interaction in the fluorogen that was responsible for red-shift in the emission spectra from 522nm (in hexane) to 750nm (in THF).

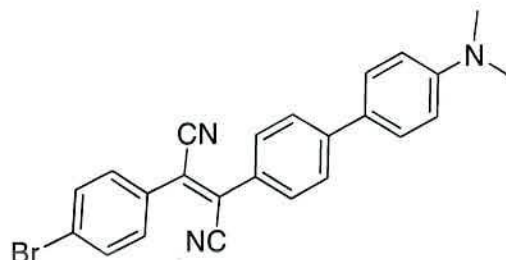


**Figure 5.** Structure of Fluorogen- BDABFN, F11

BDABFN fluorogen also exhibited twisted intramolecular charge transfer in polar solvents as the interaction between N,N-dimethyl and fumaronitrile.

**Table 2.** Photophysical study of F11 in different solvents<sup>a</sup>

Solvents	$\Delta f$	$\lambda_{ab}(nm)$	$\lambda_{em}(nm)$	Stokes shift(nm)	$\Phi_F$
Hexane	~0	437	552	115	27.3
Cyclohexane	~0	443	559	116	27.7
Toluene	0.014	455	640	185	29.3
1,4-dioxane	0.021	443	666	223	12.9
Choloroform	0.149	463	690	227	4.8
Ethyl acetate	0.201	441	720	279	0.4
THF	0.210	445	750	305	0.4
Ethanol	0.288	445	n.d.	-	0
CAN	0.306	437	n.d.	-	0
MeOH	0.309	441	n.d.	-	0

<sup>a</sup>Abbreviations:  $\lambda_{ab}$  = absorption maximum,  $\lambda_{em}$  = emission maximum,  $\Phi_F$  = quantum yield (Rhodamine B as reference) (70% in ethanol), n.d.= not detectable. Concentration used = 10  $\mu$ M.

Zhang et al.<sup>34</sup> reported new dye nanoparticles (NPs) which are characteristically highly luminescent and showed efficient emission in near- infrared (NIR) region. These NPs as fluorescent probes used in the bio-imaging application. Fabricated NPs materials exhibited wide range of biocompatibility, high photostability and pH (4-10) stability than conventional dyes reported. Structure of dye, bis-(4-(N-(2-naphthyl)phenylamino)phenyl fumaronitrile (NPAPF, **F12**) shown in Figure 6. These NPs showed prominent aggregation induced emission (AIE) properties, which endowed this probe with high fluorescence quantum (14.9%). Intense emission peak observed at 650nm. In cell imaging application, these materials in conjugation with folic acid targeted in *vitro* cell imaging. Intense fluorescence ability of NPAPF NPs makes it distinctly selective materials to resolve tumor sites in exposure time of 5ms. Overall analysis of these NPs makes them potential functionalize materials for in-vivo and in- vitro diagnosis.

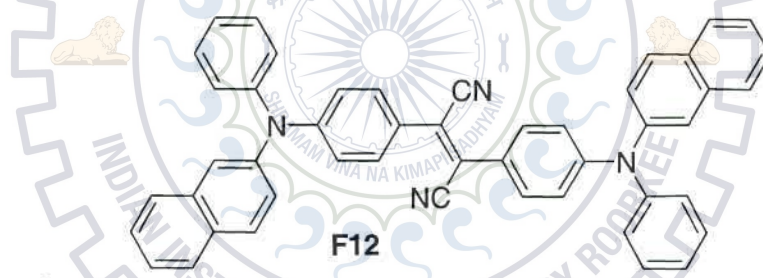


**Figure 6.** Structure of NPAPF, **F12**

Another advantage of the NPAPF NPs is that it exhibit large stokes shift (of 175 nm) in photophysical analysis, excitation at 475 nm showed intense emission at 650 nm. So that auto fluorescence reduced during excitation and emission which lead to sensitivity.<sup>35</sup>

Tang and co-workers<sup>36</sup> recently synthesized tetraphenylethene (TPE)-fumaronitrile based materials as 2,3-bis(4'-(1,2,2-triphenylethenyl)biphenyl-4-yl) fumaronitrile (BTPEFN, **F13**) and 2,3-bis(4'-(2,2-bis(4-(diethylamino)phenyl)-1-phenylethenyl)-biphenyl-4-yl) fumaronitrile

(BATPEFN, **F14**). Structures of dyes (**F13** and **F14**) shown in Figure 7. Mainly motive of this group was to study the effect of substituents on donor-acceptor systems of TPE-fumaronitrile. TPE derivatives (**F13**, **F14**) are the most attractive species for their AIE performance, facile synthesis, and flexible structure modification. BTPEFN film showed orange fluorescence with intense emission at 575nm with 100% quantum yield ( $\Phi_F$ ). Due to two cyano groups in the center of BTPEFN -

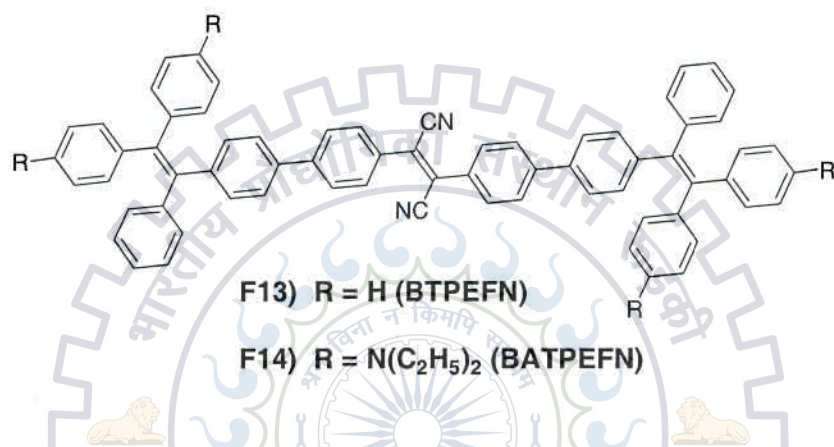


**Figure 7.** Structure of **F13** (BTPEFN) and **F14** (BATPEFN)

evidently showed intramolecular charge transfer property so that change in the emission color from green to reddish-orange on changing the solvent property from hexane to THF. While BATPEFN showed dramatically change in the fluorescence at higher red-shift (713nm) because of intramolecular charge transfer and enhanced solvatochromism.

Brad et al.<sup>37</sup> reported highly prominent red fluorophore as diphenylamino-spiro-bifluorenyl fumaronitrile (FPhSPFN, **F15**) Figure 8. This dye shows electrogenerated chemiluminescence (ECL). Dye contains two diphenylamino groups as strong donor and fumaronitrile as strong acceptor, D-A linked through spiro-bifluorene as linker. In electrochemical study, two one-electron transfer reduction waves and single two-electron

transfer oxidation wave observed which were separated by 63mV. There was a wavelength shift of 35nm in ECL spectrum in comparison with photoluminescence (PL) spectrum. In ECL spectrum intense peak was observed at 708nm with a red-shifted shoulder at 750nm. ECL study was done in benzene:acetonitrile mixture.

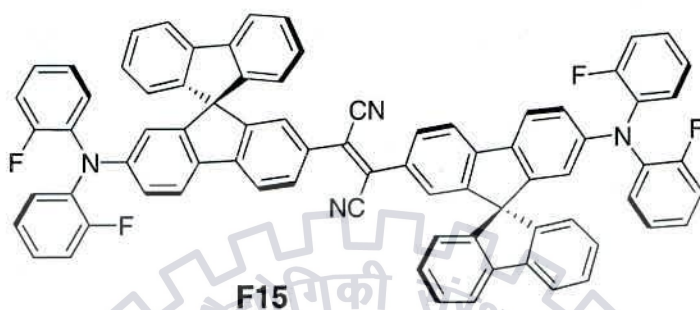


**Figure 8.** Structure of **F15** (FPhSPFN)

Zhang et al.<sup>38</sup> synthesized a dye, bis(4-(N-(9,9-diethyl-2-fluorenyl)-3,5-dimethylphenylamino)phenyl) fumaronitrile shown in Figure 9 (FMPAFN, **F16**) and showed intense red fluorescence and used as a promising material in non-doped electroluminescent devices. EL device with three layer of **F16** showed intense emission at 680nm and with four layer showed emission at 684nm. Efficiency was recorded for FMPAFN dye as 1.89. In EL devices this dye act not only as emitters but also prominent hole-transporting materials.

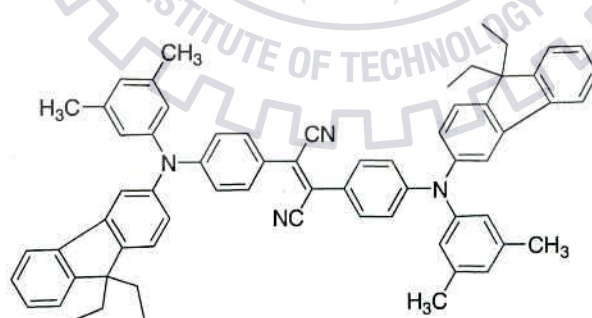


**Figure 9.** Structure of **F16** (FMPAFN)



Matsumoto et al.<sup>39</sup> reported bisazomethine dyes from diaminomaleonitrile, aminobenzaldehydes and 2,3-bis[(*E*)-4-(dialkylamino)benzylideneamino] fumaronitrile derivatives and these dyes showed potentiality for forming J-aggregate vapour-deposited films. These dyes (**F17-F24**) are shown in Figure 10. In their work, they studied the effect of alkoxy substitution on the crystal structure of 2,3-bis[(*E*)-4-(diethylamino)-2-alkoxybenzylideneamino]fumaronitrile derivatives by characterizing pure J-aggregates of bisazomethine dyes in crystalline state through analysis of two-dimensional molecular stacking layer and its alignment. As the alkoxy substitution chain length increased resulting no any significant structural change in the stacking layer.

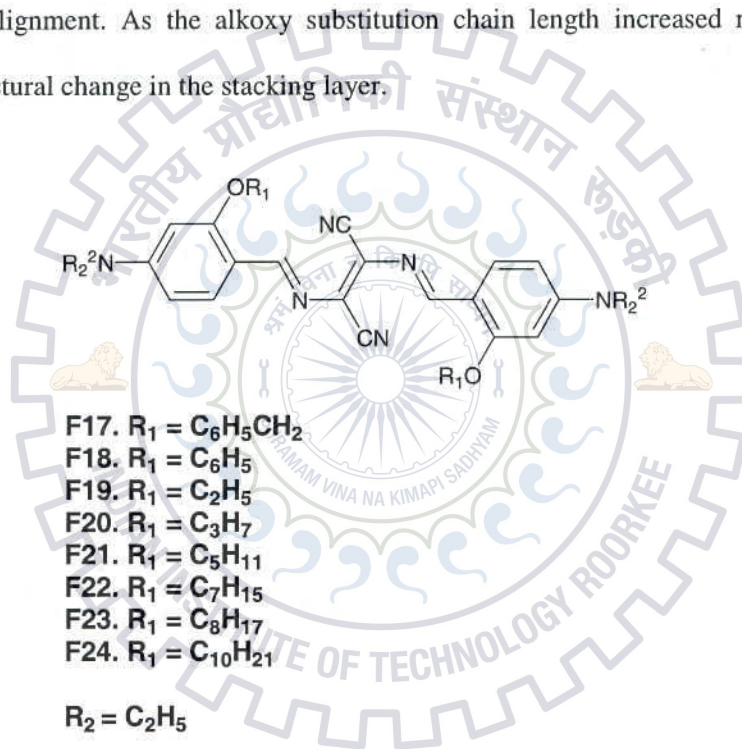


**Figure 10.** Structure of bisazomethine dyes (**F17-F24**)

### 1.3 Acrylonitrile based functionalized organic materials

Douglas C. Neckers et al.<sup>40</sup> reported a dye, 1-cyano-tarns-1,2-bis-(4-carbazolyl)phenylethylene (CN-CPE, **F25**) in crystals form and structure shown in Figure 11, which produced enhanced aggregation- induced emission. In the crystallographic analysis found high luminescence efficiency in the CN-CPE crystals. High efficiency of the dye was due to the intermolecular hydrogen bonding, lack of supramolecular interaction and  $\pi$ - $\pi$  alignment in the molecule. These were the important keys factors responsible for AIEE in CN-CPE with rigid twisted confirmation. Due to enhanced aggregation induced emission, CN-CPE exhibited intense fluorescence in solid state.

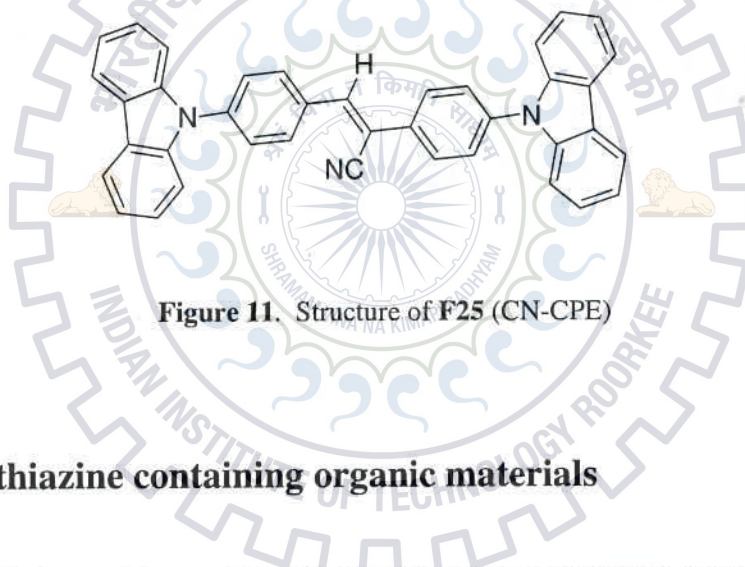


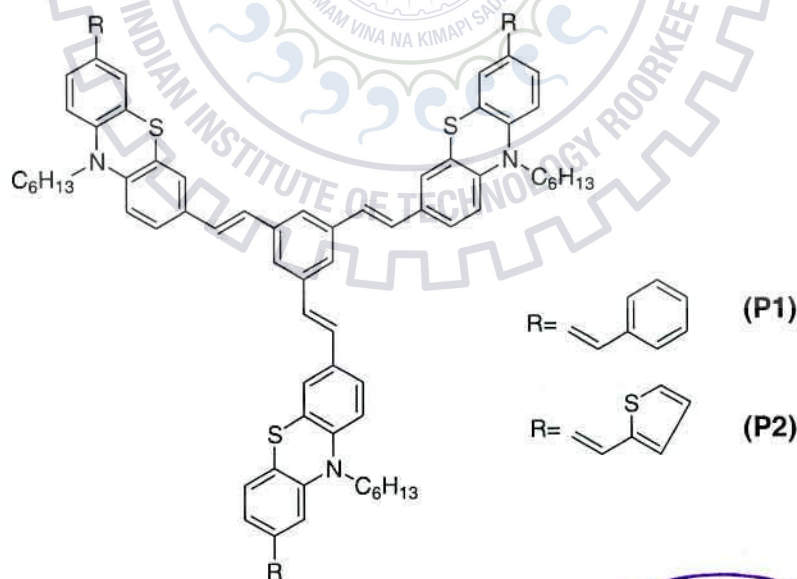
Figure 11. Structure of **F25** (CN-CPE)

### 1.4 Phenothiazine containing organic materials

Phenothiazine moiety contains electron-rich sulfur and nitrogen heteroatoms. So, it is well known as electron donating species and stable radical cation can be easily formed due to low oxidation potential.<sup>41</sup> In comparison to carbazole and fluorene, phenothiazine much promising moiety due to its butterfly shaped structure provide great stability and non-polar ring in molecule. Such kind of the properties of phenothiazine can be impede the molecular

aggregation and the formation of intermolecular excimers, which may lead to promising optoelectronics properties.<sup>42</sup> Recently, some of the useful phenothiazine based spectroscopic probes were reported as spectroscopic probes in the application to study the photo-induced electron transfer.<sup>43,44</sup> Phenothiazine used as a strong electron donor species in the field of materials engineering because of their low reversible oxidation potential and widely used to synthesize the donor-acceptor organic system for electronic and optoelectronic devices.<sup>45,46</sup> In donor-acceptor system like phenothiazine- phenylquinoline based organic system, in which phenothiazine as a strong donor and phenylquinoline group as a strong acceptor and exhibiting efficient ECL.<sup>41,47</sup>

Zhang and co-workers<sup>48</sup> synthesized a novel series of conjugated dendrimers **P1-P3** (Figure 12) through Wittig-Horner reaction and these dendrimers containing phenothiazine (at periphery) and phenylenevinylene (as core) and showed good absorption and fluorescence. Also showed larger Stokes shift due to planarity in the molecule in excited state. More conjugations in dendrimers responsible for high fluorescence efficiency



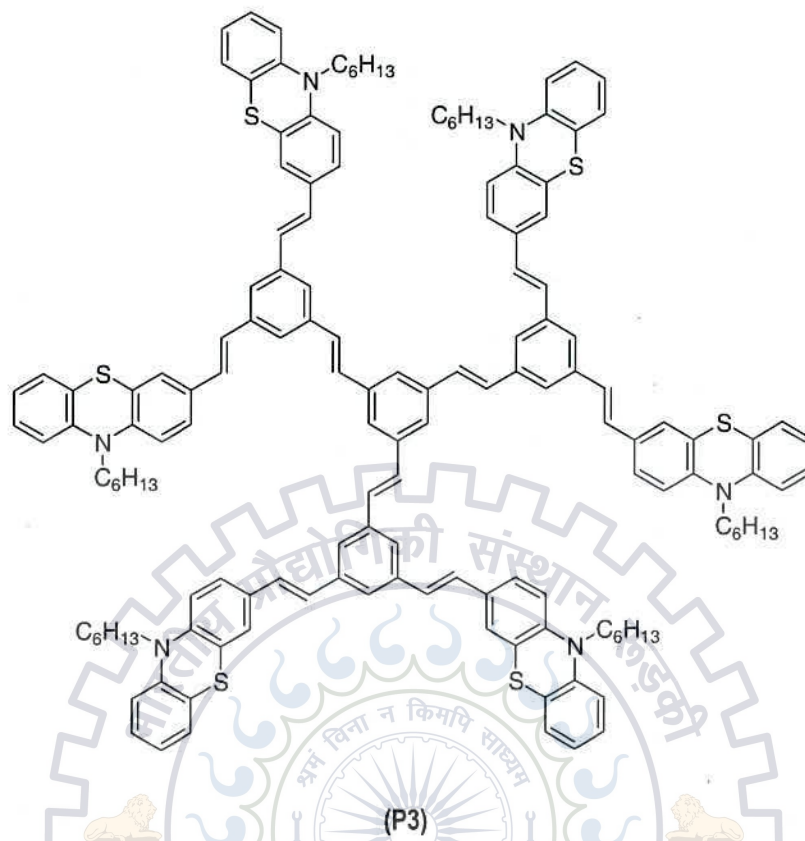
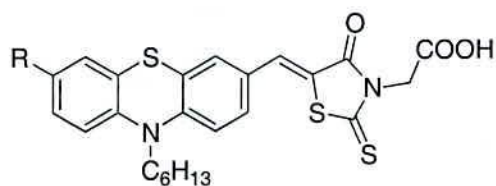


**Figure 11.** Structure of the dendrimers **P1-P3** containing vinylphenothiazine chromophores

Muller groups<sup>49</sup> reported the synthesis and photophysical, electrochemical analysis of merocyanine based dyes (**P4-P6**) shown in Figure 12. These dyes composed of D- $\pi$ -A system containing phenothiazine as electron donor moiety and rhodanylidene acetic acid as strong electron acceptor. In these D- $\pi$ -A systems, phenothiazine units contained electron rich and electron deficient groups which affected the photophysical and electrochemical properties of the whole organic system. A electron withdrawing group in the system reduced the electron density in the phenothiazine environment, which responsible for oxidation of the dye. Cyanide group in the system and conjugation in the system influences the absorption band as red-shifted.



**R = H (P4)**

**R = CN (P5)**

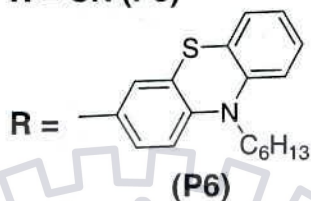


**Figure 12.** Structure of the phenothiazinyl-rhodanylidene acetic acid-merocyanines dyes (**P4-P6**)

Double donor-acceptor branched dyes (**P7-P9**) shown in Figure 13. **P7-P9** synthesized by Cao et al.<sup>50</sup> In these dyes phenothiazine units as a donor and 2-cyanoacrylic units as a acceptor and highly useful in DSSCs applications. All these dyes showed intense absorption band at 430 nm to 450 nm which is due to  $\pi-\pi^*$  transition with donor to acceptor charge-transfer character. The molar extinction coefficients of these dyes were very high and 4.22% efficiency recorded for **P8**. These branched dyes showed higher degree of emission efficiency so as promising for DSSCs application.

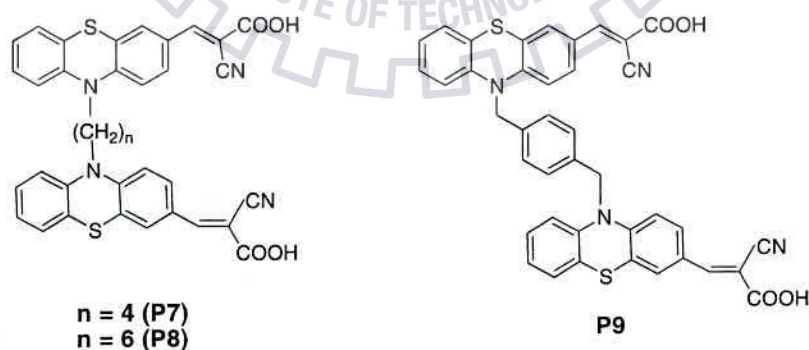


**Figure 13.** Structure of the dyes **P7-P9** containing two donors and two acceptors groups

Xie et al.<sup>51</sup> reported the synthesis and characterization of two novel organic dyes **P10** and **P11** shown in Figure 14, contains phenothiazene as electron rich species as donor and oligothiophene vinylene as conjugation spacer and cyanoacrylic acid as acceptor. In PV (photovoltaic) study they found that organic dyes with three or more conjugation units weakened the photovoltaic (PV) performance of the DDSCs because of aggregation in the dyes molecule.

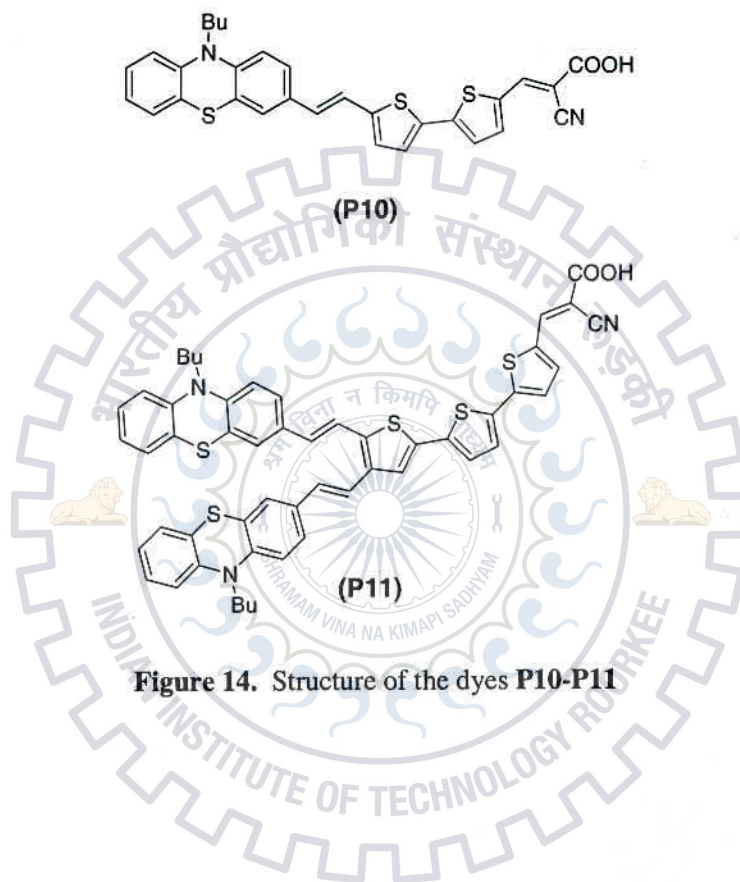


Figure 14. Structure of the dyes P10-P11

## 1.5 Aim and scope

From the above survey it is clearly evident that fumaronitrile and phenothiazine units are the promising building blocks for the construction of molecular materials for the application in electronic devices such as organic light emitting diodes (OLEDs) and dye-sensitized solar cells (DSSCs). In detail survey, we conclude that integration of phenothiazine donor with electron-deficient species fumaronitrile, is a modular approach to obtain dipolar materials, which possessing balanced charge transport and good emission characteristics. Usually phenothiazine alone exhibit poor emission due to their low oxidation potential. However, incorporation of electron-withdrawing group such as cyano has been found that enhance the photophysical properties. Likewise, fumaronitrile has two cyano group which may enhance the emission efficiency in corporation with phenothiazine moiety. Our aim to synthesize 2,3-diphenyl fumaronitrile –phenothiazine dyads and study its photophysical properties. Also, to study the effect of cyano group on photophysical properties by comparing photophysical data of fumaronitrile-phenothiazene dyads and acrylonitrile-phenothiazine dyads.

# Synthesis and characterization of 2,3-diphenyl fumaronitrile and phenothiazine dyads

## 2.1 Materials and methods

All commercially available materials were used as required for synthesis and characterization obtained from their sources. Dichloromethane (DCM) and toluene were distilled from phosphorus pentoxide and tetrahydrofuran (THF) and dimethyl formamide (DMF) distilled from sodium metal. All chromatographic separations were carried out with hexane:DCM mixture on silica gel (100-200 mesh, Rankem)

NMR spectral study for synthesized molecules (JK-1-8, JK-1-12 and JK-1-20) was done on Bruker AV 500 spectrometer. Operating frequency used 500 and 125 MHz in  $\text{CDCl}_3$  and  $(\text{CD}_3)_2\text{SO}$  (DMSO) respectively. Coupling constant ( $J$ ) in Hz and chemical shift ( $\delta$ ) in ppm. and  $\text{Me}_4\text{Si}$  (TMS) at 0.00ppm served as internal standard. Signals for  $\text{CHCl}_3$  ( $^1\text{HNMR}$ ,  $\delta = 7.26$  and  $^{13}\text{C NMR}$ ,  $\delta = 77.36$ ) and for DMSO ( $^1\text{HNMR}$ ,  $\delta = 2.5$  and  $^{13}\text{C NMR}$ ,  $\delta = 40.45$ ).

Infra-red spectral study was done on Nexus FTIR (Thermo Nicolet) spectrophotometer and analytical grade KBr used for pallet formation. For absorption spectral study Agilent (Carry series) UV-Vis spectrophotometer and absorption study was done with different solvents (DCM, toluene, THF, DMF, Methanol and cyclohexane). Emission spectral study was done on Shimadzu spectrofluorimeter. The samples were excited either at 340 nm (coumarin 1 reference)



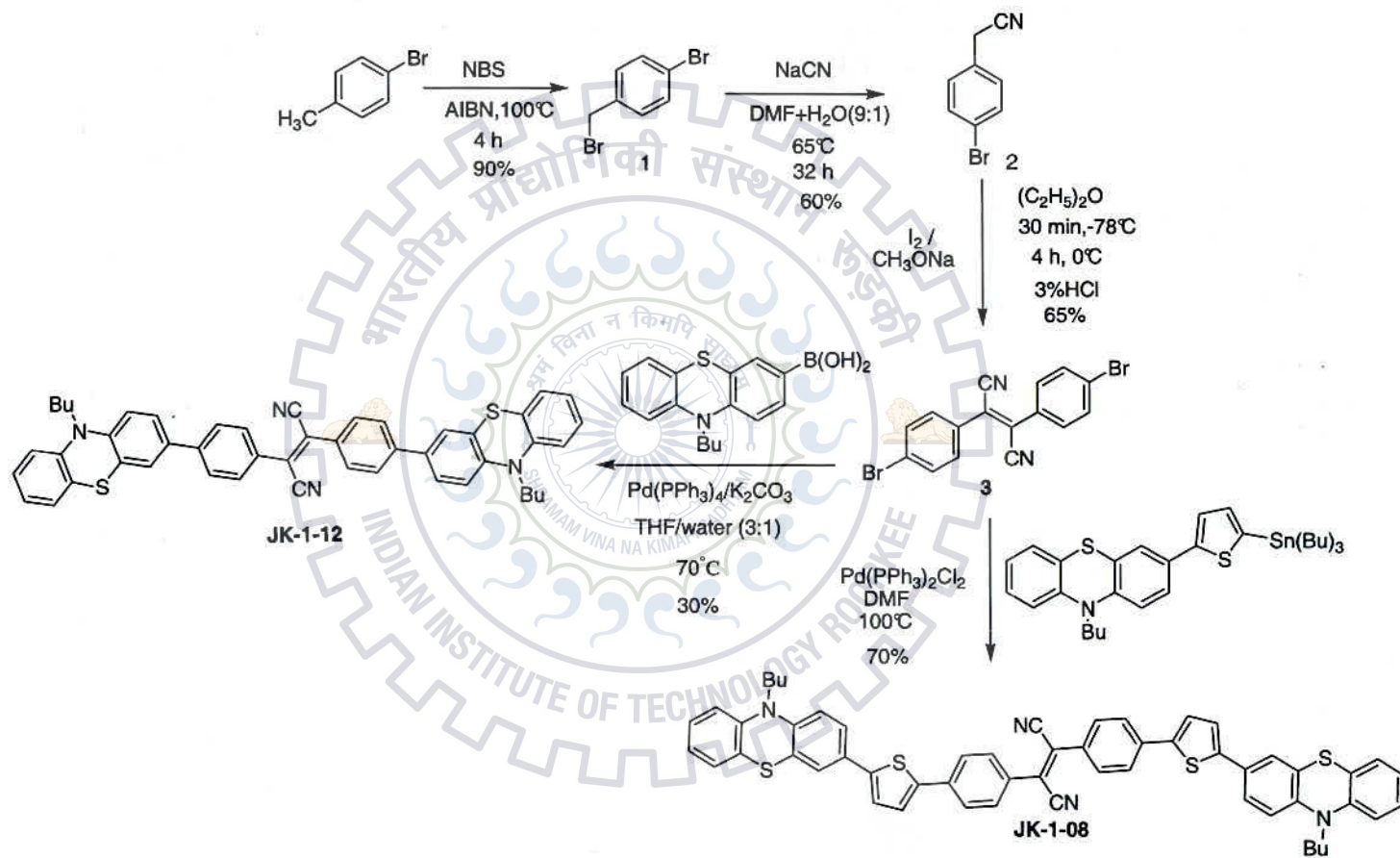
or 420 nm (for coumarin 6 reference) during the quantum yield measurements. Qualitative emission spectra of the samples were obtained by exciting at absorption maxima.

Thermal studies were performed on Perkin-Elmer (Pyris-Diamond) and TGA-DTA and DTG measurements taken at heating rate of 10 °C/min under nitrogen atmosphere.

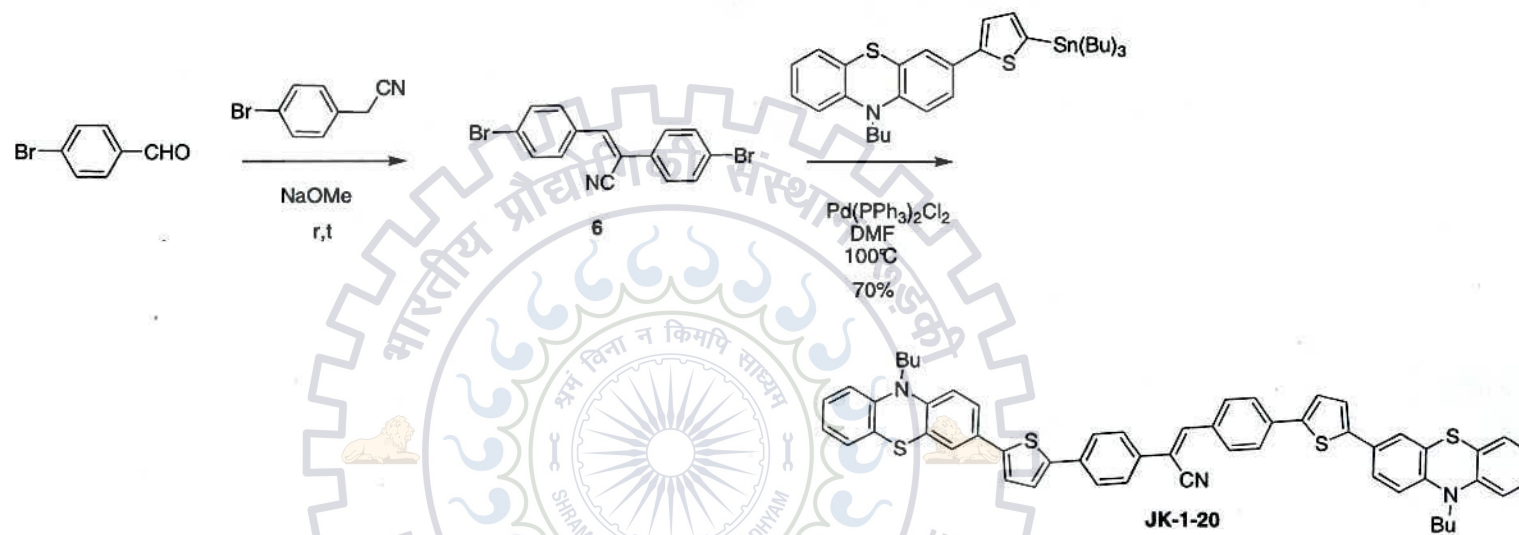
## 2.2 Synthesis of compounds

The compounds were synthesized as illustrated in synthetic Scheme 1 for 2,3-diphenyl fumaronitrile and phenothiazine dyads (JK-1-08 , JK-1-12) and synthetic scheme 2 for 2,3-diphenyl acrylonitrile and phenothiazine dyads (JK-1-20). The starting materials were required for the synthesis of compounds of interest, 1-bromo-4-(bromomethyl)benzene,<sup>52</sup> 2-(4-bromophenyl)acetonitrile,<sup>53</sup> 2,3-bis(4-bromophenyl)but-2-enenitrile,<sup>54</sup> 2,3-bis(4-bromophenyl)acrylonitrile,<sup>40</sup> were obtained by following the methods mentioned in literature. All other required chemicals and solvents were purchased from commercial source and used them after prior purification by standard methods.

Synthetic Scheme-1



## Synthetic Scheme-2



## Synthesis and characterization

### **2,3-bis(4-(5-(10-butyl-10H-phenothiazin-3-yl)thiophen-2-yl)phenyl)fumaronitrile**

**(JK-1-08):** 2,3-bis(4-bromophenyl)fumaronitrile (0.5 g, 1.3 mmol) and 10-butyl-3-(5-(tributylstannyl)thiophen-2-yl)-10H-phenothiazine (2.86 g, 2.86 mmol) in DMF (15mL) were taken in a 100 mL round bottom flask to this nitrogen was purged followed by addition of Pd(PPh<sub>3</sub>)<sub>2</sub>Cl<sub>2</sub> (14mg) and heated at 95°C for 32 h in nitrogen atmosphere. After completion of reaction the reaction mixture was diluted with dichloromethane washed with water and brine sol. The organic layer was separated, dried over Na<sub>2</sub>SO<sub>4</sub> and evaporated by rotary evaporator and crude reaction mixture was purified by column chromatography with 100-200 silica mesh, hexane/dichloromethane as eluant; Dark Brown solid; yield 0.57g (80%); M.pt: 185-188 °C. <sup>1</sup>H NMR (CDCl<sub>3</sub>, 500.13 MHz) δ p.p.m.:0.95 (t, *J* = 7.5 Hz, 3H), 1.41-1.49 (m, 2H), 1.77-1.83 (m, 2H), 3.86 (t, *J* = 7.0 Hz, 2H), 6.84-6.88 (m, 4H), 6.91-6.94 (m, 2H), 7.13-7.18 (m, 8H), 7.323 (m, *J* = 4.0 Hz), 7.38-7.40 (m, 4.0 Hz), 7.56 (d, *J* = 8.5 Hz), 7.61 (d, *J* = 8.5 Hz). <sup>13</sup>C NMR (CDCl<sub>3</sub>, 125.77 MHz) δ p.p.m.:18.80, 24.60, 33.49, 51.42, 121.00, 121.18, 127.81, 128.03, 128.61, 129.43, 129.55, 129.84, 130.01, 131.07, 132.34, 132.92, 135.66, 139.74, 140.56, 145.95, 147.85, 149.39, 149.47, 176.61.

**2,3-bis(4-(10-butyl-10H-phenothiazin-3-yl)phenyl)fumaronitrile (JK-1-12):**

2,3-bis(4-bromophenyl)-fumaronitrile (0.5 g, 1.3 mmol) and 10-butyl-10H-phenothiazin-3-ylboronic acid (0.90 g, 3.25 mmol), and potassium carbonate (0.90 g) were dissolved in 30 mL THF/H<sub>2</sub>O (3:1) stirred 10 min, to this nitrogen was purged followed by the addition of Pd(PPh<sub>3</sub>)<sub>4</sub> (75 mg) and refluxed at 100°C for 24 h in nitrogen atmosphere. After completion of reaction, reaction mixture was diluted with dichloromethane (100 mL) washed with water, the organic layer was separated dried over Na<sub>2</sub>SO<sub>4</sub> and evaporated by rotary evaporator, the crude reaction mixture was purified by column chromatography with 100-200 silica mesh and ethyl acetate/ hexane (9:1) as eluant; brownish powder; yield 200 mg (30%); M.pt: 114-116 °C. <sup>1</sup>H NMR (CDCl<sub>3</sub>, 500.13 MHz) δ p.p.m.: 0.96 (t, *J* = 7.0 Hz), 1.46-1.50 (m, 2H), 1.79-1.84 (m, 2H), 3.88 (t, *J* = 7.0 Hz), 6.87-6.94 (m, 6H), 7.13-7.17 (m, 4H), 7.38-7.40 (m, 4H), 7.53-7.60 (m, 8H). <sup>13</sup>C NMR (CDCl<sub>3</sub>, 125.77 MHz) δ p.p.m.: 14.18, 20.21, 29.74, 47.23, 115.44, 115.57, 122.56, 124.30, 125.07, 125.35, 125.70, 126.30, 126.47, 126.53, 127.03, 127.35, 127.50, 130.43, 131.46, 132.01, 134.06, 136.07, 141.43, 144.88, 145.14, 170.83.

**(E)-2,3-bis(4-(5-(10-butyl-10H-phenothiazin-3-yl)thiophen-2-yl)phenyl)acrylonitrile (JK-1-20):** (E)-2,3-bis(4-bromophenyl)acrylonitrile (0.50 g, 1.4 mmol), 10-butyl-3-(5-(tributylstannyl)thiophen-2-yl)-10H-phenothiazine (2.31 g, 3.0 mmol) in DMF (15mL) were taken in a 100 mL round bottom flask to this nitrogen was purged followed by addition of Pd(PPh<sub>3</sub>)<sub>2</sub>Cl<sub>2</sub> (14mg) and heated at 95°C for 32 h in nitrogen atmosphere. After completion of reaction the reaction mixture was diluted with dichloromethane washed with water and brine sol. The organic layer was separated, dried over Na<sub>2</sub>SO<sub>4</sub> and evaporated by rotary evaporator and crude reaction mixture was purified by column chromatography with 100-200 silica mesh, hexane/dichloromethane as eluant: orange solid; yield 0.60 g (60%); M.pt: 216-218 °C. <sup>1</sup>H NMR (CDCl<sub>3</sub>, 500.13 MHz) δ p.p.m.: 0.96 (t, *J* = 7.5 Hz), 1.46-1.50 (m, 2H), 1.78-1.84 (m, 2H), 3.87 (t, *J* = 7.0 Hz), 6.85-6.89 (m, 4H), 6.91-6.94 (m, 2H), 7.14-7.16 (m, 4H), 7.18-7.21 (m, 2H), 7.34 (d, *J* = 4 Hz, 1H), 7.37-7.41 (m, 5H), 7.53 (s, 1H), 7.67-7.71 (m, 6H), 7.94 (d, *J* = 8.0 Hz).

# Photophysical analysis of 2,3-diphenyl fumaronitrile and phenothiazine dyads

## 3.1 Introduction

Now a days, donor-acceptor organic system with  $\pi$ -conjugation extensively synthesized and photophysically analyzed because of their high efficiency (quantum yield) and in wide scope these system used in electronics and optoelectronics devices such as dye sensitized solar cells (DSSCs), organic light-emitting diodes (OLEDs), non-linear optics, ECL application and photovoltaic cells,<sup>55</sup> also used as chemo- and bio-sensors. Unique structure of donor-acceptor systems permits the alteration in photophysical and electrochemical properties by variation in functional group as structural changes by chemical modification in the donor and acceptor group. Donor-acceptor compounds were also synthesized to unravel the electronic interaction between them to establish the structural properties relationship of those molecules. In this report we represent the syntheses of two series of D-A molecules in which phenothiazine act as donor and fumaronitrile as strong acceptor. Additional group such as thiophene, phenyl ring have been used to extend the  $\pi$ -conjugation of the phenothiazine nucleus. We describe herein the photophysical and thermal characteristics of the newly synthesized functional materials.

All the dyes are thoroughly soluble in common organic solvents such as toluene, DCM, THF, DMF, etc. These compounds are solid brown (JK-1-8, JK-1-12) and solid intense orange (JK-1-20) in color. In the solution state solid brown dyes turned into reddish color and orange dye turned into intense yellow color. The structural compositions of the all compounds were established by routine  $^1\text{H}$  NMR and  $^{13}\text{C}$  NMR spectral measurements. (See supporting information)

### 3.2 Photophysical properties

Absorption study of the dyes JK-01-8, JK-01-12, and JK-1-20 recorded in dichloromethane and displayed in Figure 1. The absorption spectral data compiled in Table 1. However, except JK-1-12 all the dyes are exhibited two absorption peaks, the absorption peak at higher energy is corresponding to phenothiazine localized  $\pi-\pi^*$  transition and peak at lower energy represents charge transfer (CT) from donor to acceptor. Here phenothiazine act as a donor and fumaronitrile and acrylonitrile act as acceptor and the absorption spectra represents all the dyes have good donor-acceptor (D-A) architecture.

**Table 1.** Photophysical properties of the dyes recorded in DCM (dichloromethane)

Dyes	$\lambda_{\text{abs}}$ , nm ( $\epsilon_{\text{max}} \times 10^3 \text{ M}^{-1} \text{ cm}^{-1}$ )	$\lambda_{\text{em}}$ , nm	Stokes shift/ $\text{cm}^{-1}$
JK-1-08	332(41.6), 455(sh)	544	3596
JK-1-12	423(11.3)	500	3641
JK-1-20	335(37.0), 435(67.7)	570	5445



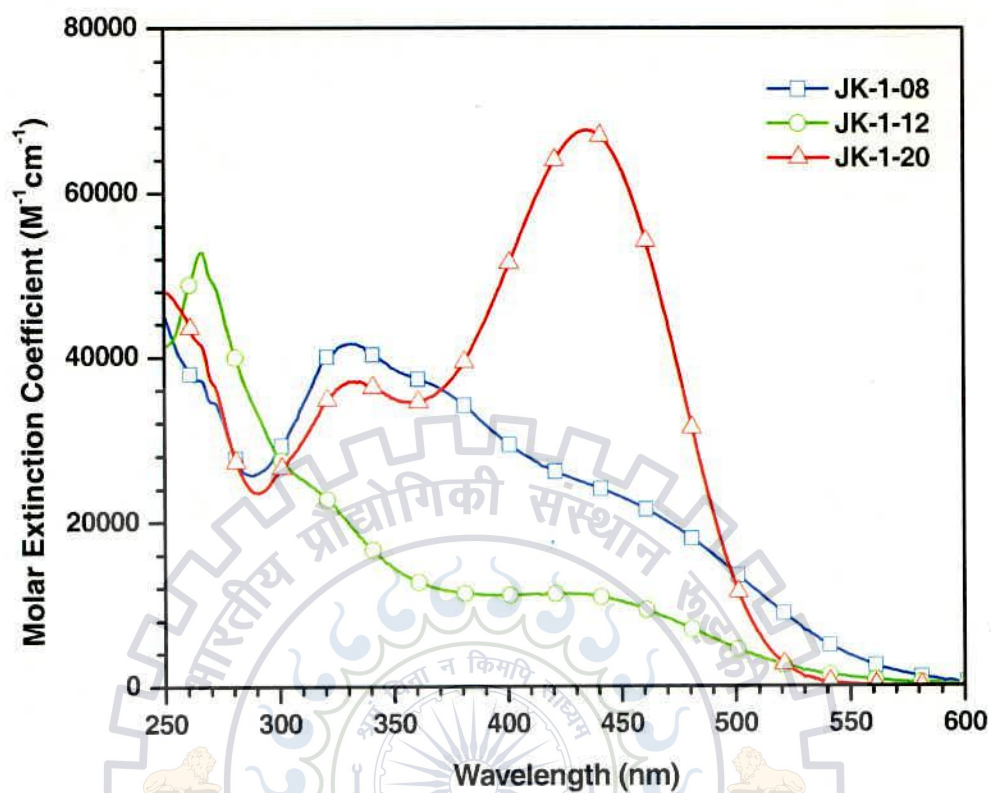


**Figure 1.** Absorption spectra of the dyes recorded in dichloromethane

In order to predict ground state nature of dyes, the absorption spectra of all the dyes recorded with increasing solvent polarity from cyclohexane to *N,N*-dimethylformamide showed in Figure 2-4 and their spectral data depicted in Table 2. Except JK-1-20 remaining all the dyes showed blue shift absorption with increasing solvent polarity, it indicates that the HOMO of all the dyes is stabilized with increasing solvent polarity.

**Table 2.** Photophysical properties of compounds in all solvents

Dyes	$\lambda_{\text{abs}}$ , nm ( $\epsilon_{\text{max}} \times 10^3 \text{ M}^{-1} \text{ cm}^{-1}$ )						$\lambda_{\text{em}}$ , nm					
	CH	TOL	DCM	THF	MEOH	DMF	CH	TOL	DCM	THF	MEOH	DMF
<b>JK-1-08</b>	a	332(40.4),	332(41.6),	330(40.4),	a	395(16.0),	563	532	544	527	536	539
		455	450(sh)	455(sh)	430(sh)	425(sh)						
<b>JK-1-12</b>	427	427(8.4)	423(11.3)	406(13.6)	406	411(sh)	572	547	500	507	495	481
<b>JK-1-20</b>	a	331(38.3),	335(37.0),	331(43.0),	a,	348(35.6),	509	553	570	574	570	549
		415	431(55.7)	435(67.7)	434(78.9)	409	440(80.2)					

a Absorption peaks was ambiguous

Among all the dyes **JK-1-08** showed red shift absorption, it is due to more extended conjugation and good donor – acceptor architecture and interestingly in the absorption spectra both absorption peaks such as  $\pi-\pi^*$  transition and CT band are merged. It indicates that dye **JK-1-08** have strong donor acceptor interactions among all the dyes and dye **JK-1-12** showed blue shift absorption due to less conjugation in the molecule. Due to weak acceptor nature of acrylonitrile chromophore compared to fumaronitrile chromophore dye **JK-1-20** showed hypsochromic shift than **JK-1-08**. Finally, the CT absorption band trend for all the dyes is as follows **JK-1-12 < JK-1-20 < JK-1-08**.

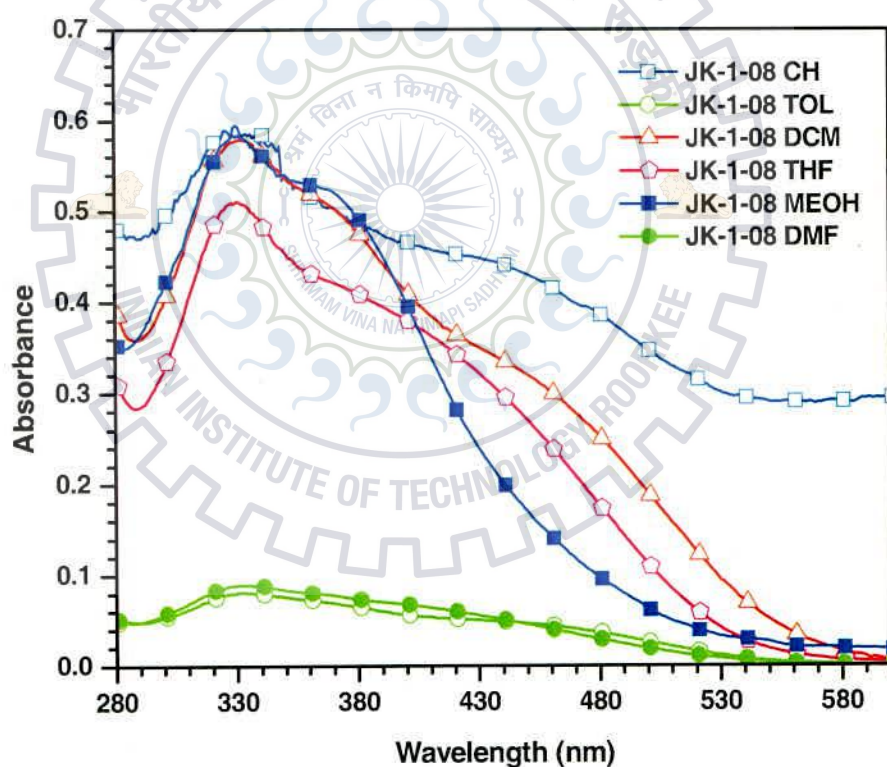


**Figure 2.** Absorption spectra of the **JK-1-08** recorded in different solvents

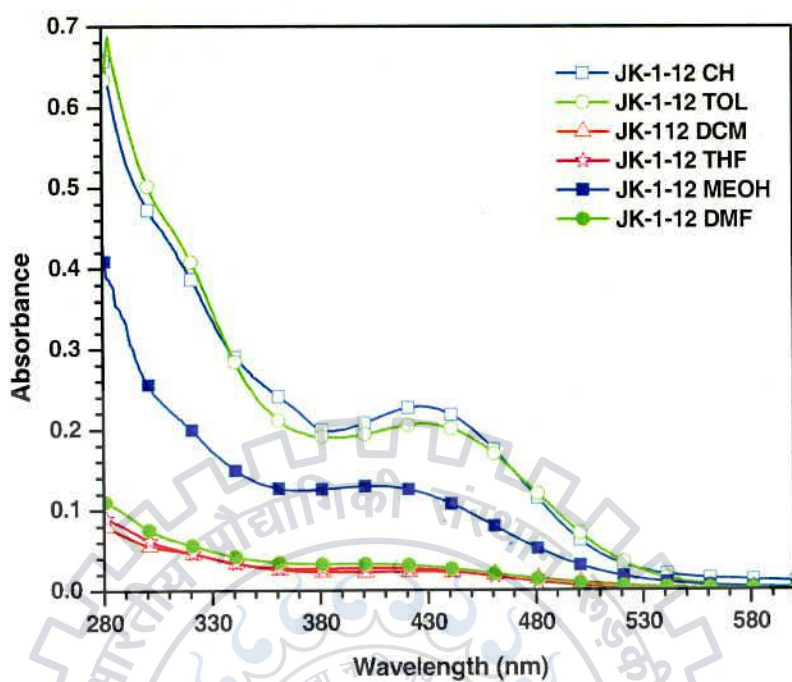


Figure 3. Absorption spectra of the JK-1-12 recorded in different solvents

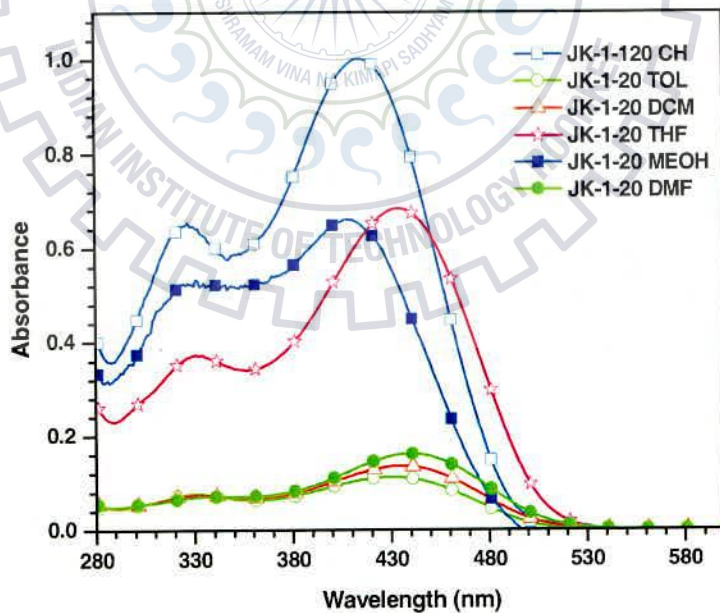
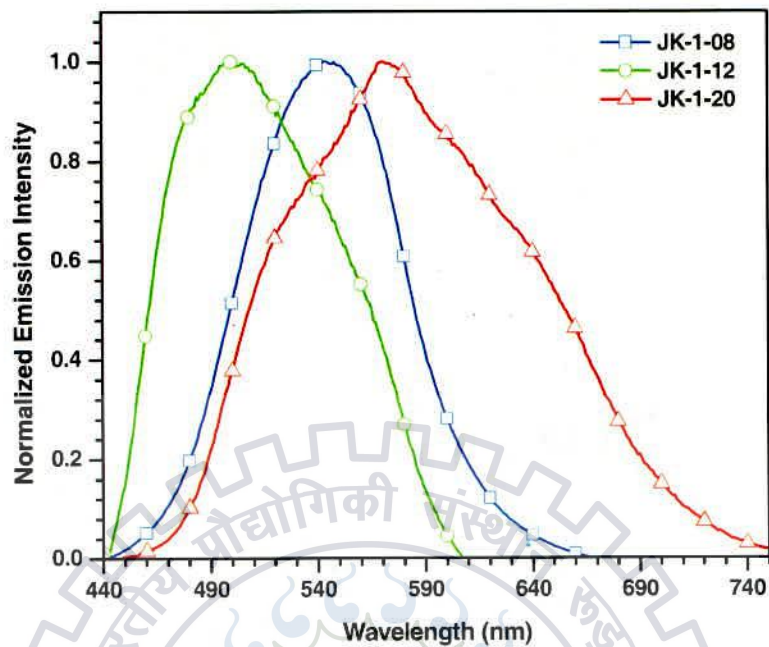


Figure 4. Absorption spectra of the JK-1-20 recorded in different solvents



**Figure 5.** Emission spectra of the dyes recorded in dichloromethane

Emission spectra of the dyes recorded in dichloromethane by measuring fluorescence spectra and displayed in Figure 5 and pertinent data are compiled in Table-2. Except dye **JK-1-20** remaining all the dyes showed emission maxima similar to absorption peak positions observed for them (Table 1). The emission maxima of the dyes follows the trend **JK-1-20 < JK-1-08 < JK-1-12** and all the dyes exhibit structure less emission profile.

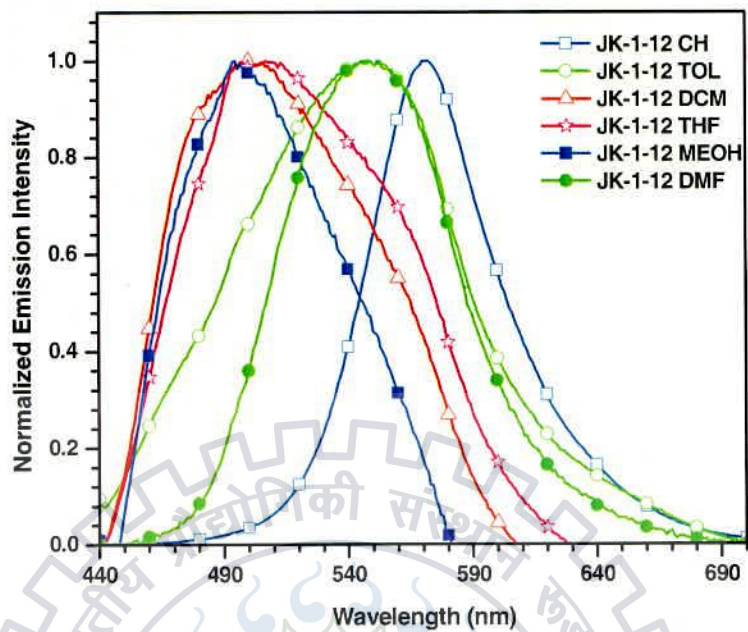


Figure 6. Emission spectra of **JK-1-12** recorded in different solvents

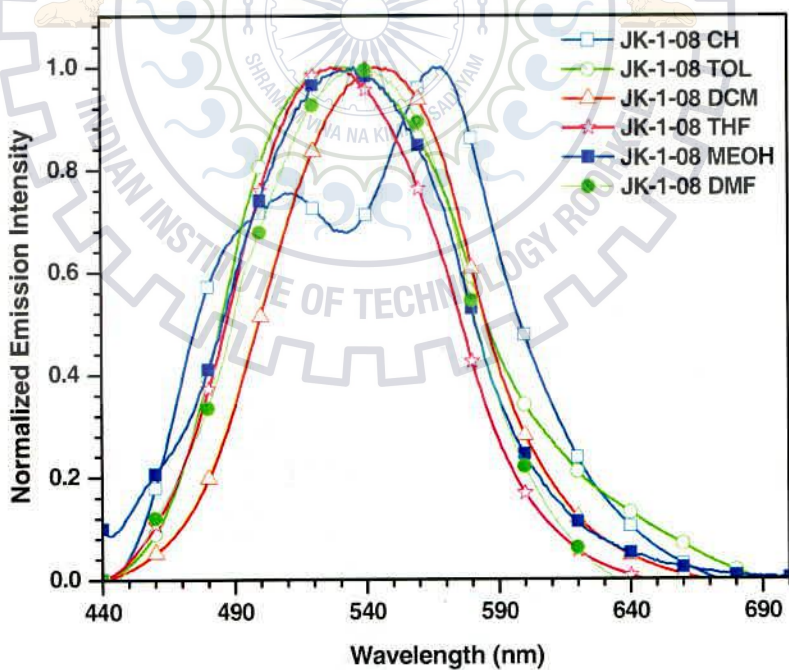


Figure 7. Emission spectra of **JK-1-08** recorded in different solvents

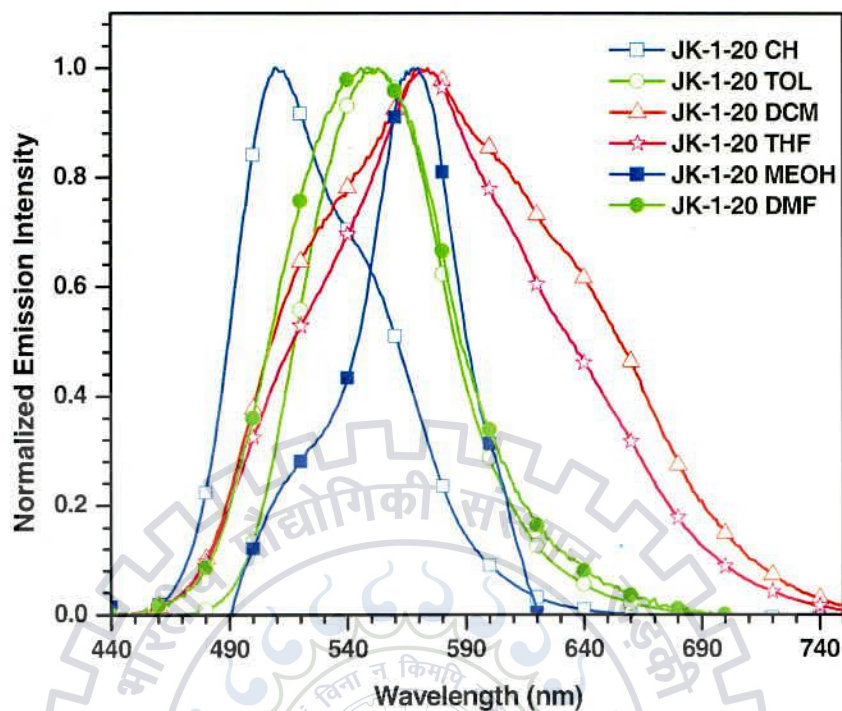


Figure 8. Emission spectra of JK-1-20 recorded in different solvents

In order to predict excited state nature of dyes the fluorescence spectra of the dyes displayed in Figure 6-8, recorded with increasing solvent polarity and their fluorescence data compiled in Table 2. Except dye JK-1-20 all the dyes showed negative solvatochromism, like absorption spectra. With increasing solvent polarity emission maxima blue shifted for JK-1-08 and JK-1-12, indicates that LUMO of the dyes destabilized. Dye JK-1-20 showed red shift emission maxima  $< 60$  nm in polar solvents such as methanol compared with non polar solvents such as cyclohexane and toluene, indicates that in the excited state showed salvation with more polar solvents. But in the case of JK-1-08 and JK-1-12 such effect was not observed, it represents that in the excited state these molecules are not showed salvation, but appearance of red shifted

emission maxima in less polar solvents such as cyclohexane and toluene indicates that these dyes are less polar in the excited state.

In the case of **JK-1-20**, we characterized solvatochromism effect due to large induced dipole moment as the charge transfer from phenothiazine electron donating unit to electron withdrawing acrylonitrile subunit. In methanol, JK-1-20 showed large stokes shift compared to the other dyes and solvents represents that there is a considerable change in the excite state. For all the dyes stokes shift compiled in Table 3

**Table 3.** Stokes shift of the dyes in different solvents

Dyes	Stokes shift/cm <sup>-1</sup>						Td, °C (5% weight loss)
	CH	TOL	DCM	THF	MEOH	DMF	
<b>JK-1-08</b>	4216	3425	3596	4280	b	4977	240
<b>JK-1-12</b>	5937	5138	3641	4907	4429	4526	248
<b>JK-1-20</b>	4450	5119	5445	5620	6906	4512	90

b= insoluble

Solvent dependent spectral properties of compounds were interpreted by using Lippert-Mataga equation, Et(30) parameter and Kamlet-Taft equation. This equation measured the change in dipole moment as upon excitation in the compounds. In this methods a plot of stokes shift versus orientation polarizability ( $\Delta f$ ) was performed to fit the equation given below:



$$\bar{\nu}_A - \bar{\nu}_F = \frac{2}{hc} \left( \frac{\epsilon - 1}{2\epsilon + 1} - \frac{n^2 - 1}{2n - 1} \right) \frac{(\mu_\epsilon - \mu_G)}{a^3} + \text{constant}$$

where  $h$  is Planck's constant ( $6.6256 \times 10^{-27}$  erg),  $c$  is the velocity of light ( $2.9979 \times 10^{10}$  cm/s),  $a$  is a radius of cavity in which molecule resides,  $\bar{\nu}_A$  and  $\bar{\nu}_F$  are the wave numbers ( $\text{cm}^{-1}$ ) of the absorption and emission respectively.  $\epsilon$  represents dielectric constant and  $n$  represents refractive index. The orientation polarizability is calculated by following equation:

$$\Delta f = \frac{2}{hc} \left( \frac{\epsilon - 1}{2\epsilon + 1} - \frac{n^2 - 1}{2n - 1} \right)$$

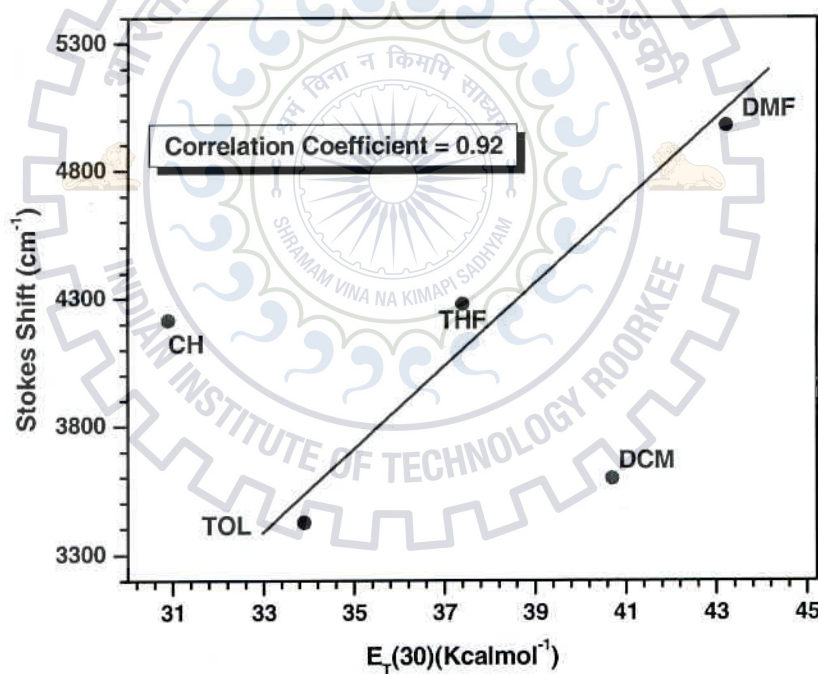


**Figure 9.** Correlation of  $E_T(30)$  parameter with Stokes shift for JK-1-08

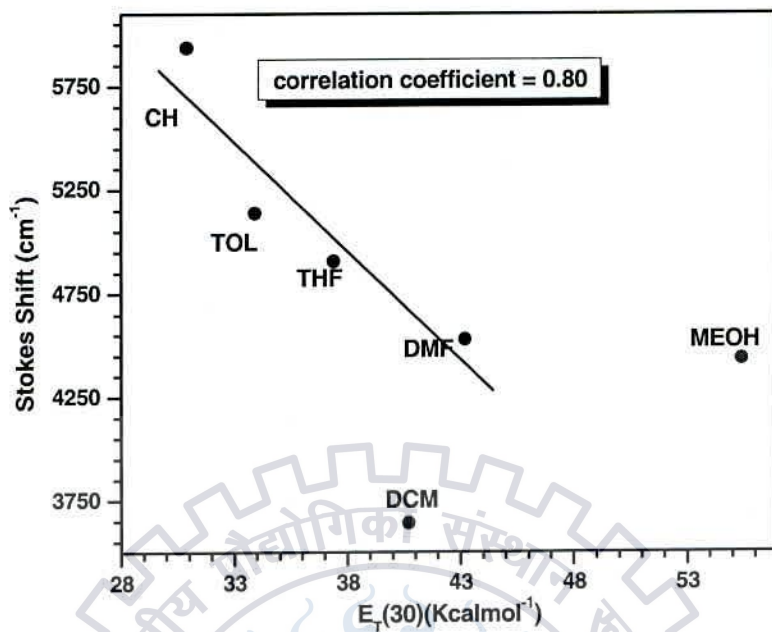


Figure 10. Correlation of  $E_T(30)$  parameter with Stokes shift for the JK-1-12

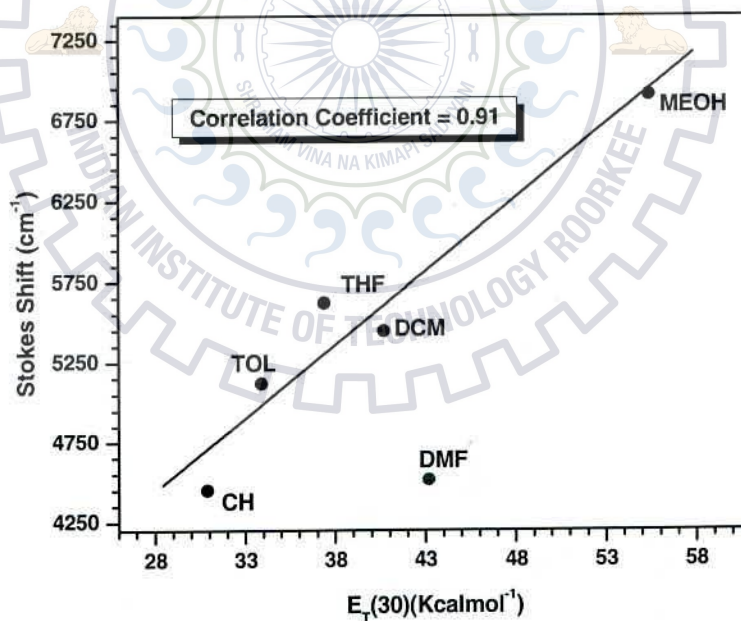


Figure 11. Correlation of  $E_T(30)$  parameter with Stokes shift for JK-1-20

For all the dyes Lippert–Mataga,  $E_T(30)$  parameter plots were plotted and they are displayed in figure 9-13. In the Lippert–Mataga plot of dye **JK-1-12** showed deviation from linearity in dichloromethane, this anomalous behavior because no specific interaction such as hydrogen bonding and aggregation was observed. Same effect was observed for **JK-1-20** in *N,N*-dimethylformamide and tetrahydrofuran.

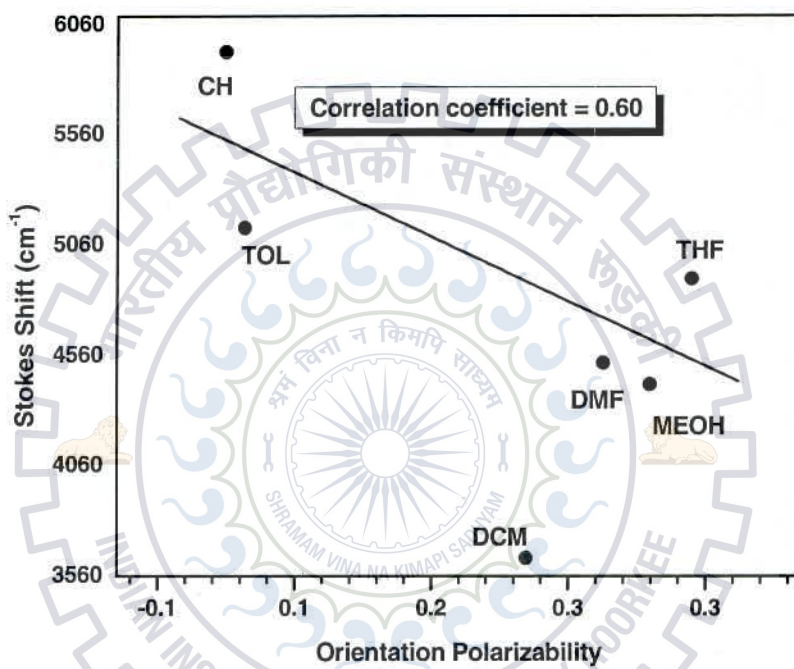


Figure 12. Lippert–Mataga plots of the dye **JK-1-12**

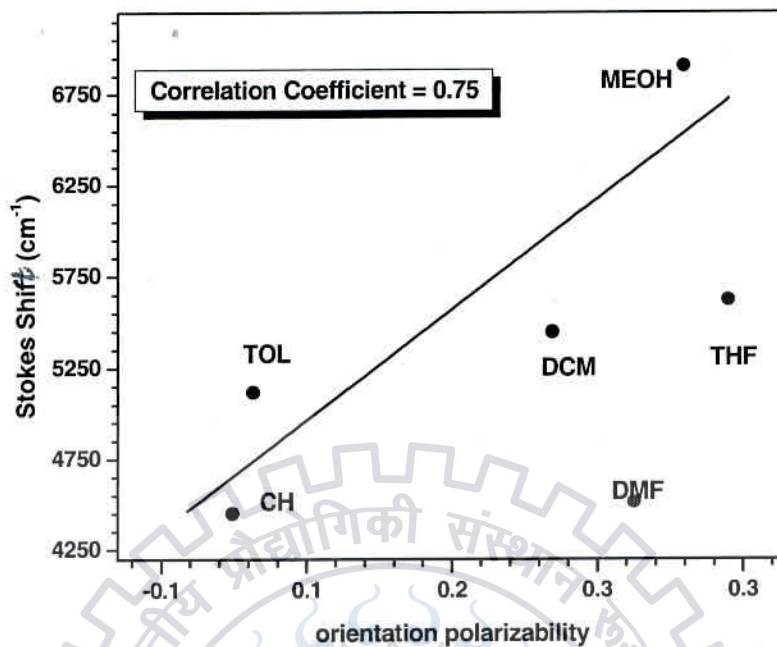


Figure 13. Lippert–Mataga plots of the dye JK-1-20

The plot of stokes shift versus the  $E_T(30)$  parameter for all the dyes displayed in Figure 9-11 based on Figure 9 and Figure 11 confirmed that JK-1-08 and JK-1-20 exhibited positive solvatochromism and based on Figure-- it is also confirmed that JK-1-12 exhibited negative solatochromism. Deviation of linearity in cyclohexane and dichloromethane of the plot of stokes shift versus the  $E_T(30)$  parameter of dye JK-1-08

### 3.3 Conclusions

Newly developed donor-acceptor compounds based on fumaronitrile and phenothiazine units have been synthesized and characterized by various spectroscopic methods. Photophysical analysis of these compounds as electronic absorption, fluorescence emission, showed the presence of significant donor-acceptor interaction between fumaronitrile acceptor and phenothiazine donor. Charge transfer band showed in absorption and emission of compounds due the direct linkage between fumaronitrile and phenothiazine. Different molecular pattern exhibited on conjugation and addition of some groups, were found to influence the optical and thermal properties of the compounds. All these inferences suggest that this can be used as an efficient method to a fine tune the electronic parameters such as LUMO levels without significantly affecting the energy levels of HOMO. Such type of new designed molecule will be beneficial to balance the electron or hole injection/transfer in the organic light-emitting devices and may also used as fluorogen in bioimaging application

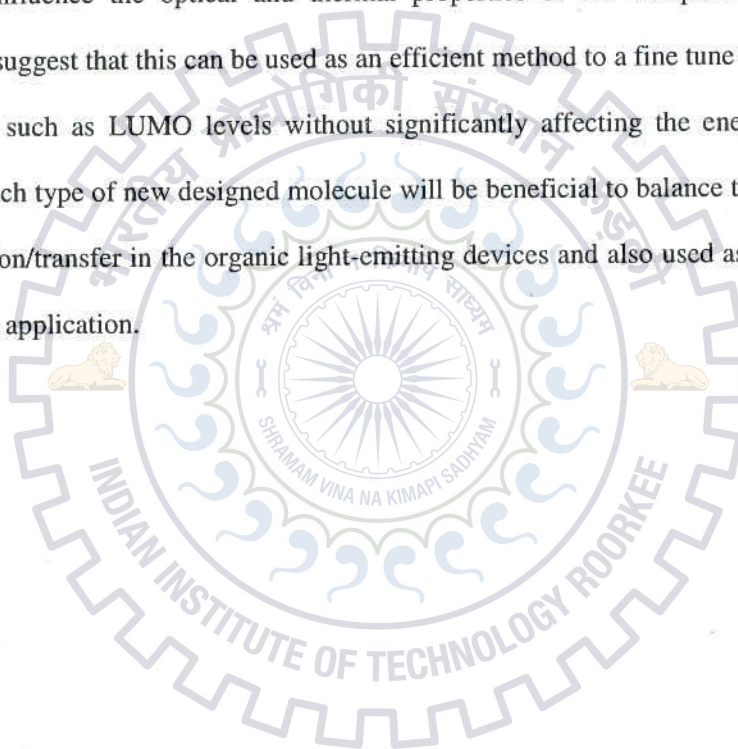
## Chapter 4

### Summary

Donor- acceptor compounds (dipolar compounds) are more attractive due to their unique properties such as red-shifted absorption and emission, highly polarized excited state. Due to these unique features eventually leads to charge separation, ordered solid state arrangements producing high conductivity properties, and balanced charge transport characteristics. Dipolar compounds containing donor fragments such as triphenylamine and carbazole and acceptor moieties such as oxadiazole, quinoxaline, pyridine, benzothiadiazole, benzotriazole etc. have been designed and their structure property relationship investigated. We hypothetically assume that the integration of easily oxidizable phenothiazine unit with a moderately electron-accepting fumaronitrile segment would resulting a new novel class of dipolar compounds exhibiting unique optical properties. We also planned to study the effect of cyanide on photophysical properties on some augmented molecular structure with additional chromophores capable of alternating the electronic structure of phenothiazine and fumaronitrile moieties. We also wish to study thermal stability of the dyes, may be promising candidates in DSSCs and OLEDs and bioimaging applications.

In this dissertation, we have presented the synthesis and characterization of new donor-acceptor compounds based on fumaronitrile (acceptor moiety) and phenothiazine (donor moiety) units. The compounds were characterized by routine spectral techniques

such as  $^1\text{H}$  and  $^{13}\text{C}$  NMR and IR and confirm their molecular composition. Electronic absorption, fluorescence emission and thermal studies of these compounds showed the presence of significant donor-acceptor interaction between fumaronitrile acceptor and phenothiazine donor. Charge transfer band in the absorption and emission spectra of these compounds due to the direct linkage between fumaronitrile and phenothiazine. Different molecular pattern exhibited on conjugation and addition of some groups, were found to influence the optical and thermal properties of the compounds. All these inferences suggest that this can be used as an efficient method to a fine tune the electronic parameters such as LUMO levels without significantly affecting the energy levels of HOMO. Such type of new designed molecule will be beneficial to balance the electron or hole injection/transfer in the organic light-emitting devices and also used as fluorogen in bioimaging application.



## References

- (1) Sheats, J. R.; Barbara, P. F. *Acc. Chem. Res.* **1999**, *32*, 191-192.
- (2) Wong, M. S.; Li, Z. H.; Tao, Y.; D'Iorio, M. *Chem. Mater.* **2003**, *15*, 1198-1203.
- (3) Morin, J. F.; Drolet, N.; Tao, Y.; Leclerc, M. *Chem. Mater.* **2004**, *16*, 4619-4626.
- (4) Leclerc, N.; Sanaur, S.; Galmiche, L.; Mathevet, F.; Attias, A. J.; Fave, J. L.; Roussel, J.; Hapiot, P.; Lemaitre, N.; Geffroy, B. *Chem. Mater.* **2005**, *17*, 502-513.
- (5) Kim, B.-S.; Jindo, T.; Eto, R.; Shinohara, Y.; Son, Y.-A.; Kim, S.-H.; Matsumoto, S. *Cryst. Eng. Comm.*, **2011**, *13*, 5374-538.
- (6) Bricaud, Q.; Cravino, A.; Leriche, P.; Roncali, J. *Synth.Met.*, **2009**, *159*, 2534-2538.
- (7) Lee, H.N.; Lee, Y.G.; Ko, I.H.; Hawang, E.C.; Kang, S.K. *Curr.Appl.Phys.*, **2008**, *8*, 620-630.
- (8) Anthony, J.E. *Chem.rev. (Washington, DC, U.S.)*, **2006**, *106*, 5028-5048.
- (9) Kumashiro, Y.; Nakako, H.; Inada, M.; Yamamoto, K.; Izumi, A; Ishihara, M. *Appl. Surf. Sci.*, **2009**, *256*, 1019-1022.
- (10) Friend, R. H.; Gymer, R. W.; Holmes, A. B.; Burroughes, J. H.; Marks, R. N.; Taliani, C.; Bradley, D. D. C.; Dos Santos, D. A.; Bredas, J. L.; Logdlund, M.; Salaneck, W. R. *Nature* **1999**, *397*, 121-128.



- (11) Jenekhe, S. A.; Osaheni, J. A. *Science* **1994**, *265*, 765-768.
- (12) Deans, R.; Kim, J.; Machacek, M. R.; Swager, T. M. *J. Am. Chem. Soc.* **2000**, *122*, 8565-8566.
- (13) Chen, J.; Xu, B.; Ouyang, X.; Tang, B. Z.; Cao, Y. *J. Phys. Chem. A* **2004**, *108*, 7522-7526.
- (14) Mondal, R.; Shah, B. K.; Neckers, D. C. *J. Org. Chem.* **2006**, *71*, 4085.
- (15) An, B.-K.; Kwon, S.-K.; Jung, S.-D.; Park, S. Y. *J. Am. Chem. Soc.* **2002**, *124*, 14410.
- (16) Yeh, H.-C.; Yeh, S.-J.; Chen, C.-T. *Chem. Commun.* **2003**, 2632.
- (17) Chen, C.-T. *Chem. Mater.* **2004**, *16*, 4389.
- (18) Chaskar, A.; Chen, H.F.; Wong, K.T. *Adv. Mater.*, **2011**, *23*, 3876-3895.
- (19) Jeon, S.O.; Jang, S.E.; Son, H.S.; Lee, J.Y. *Adv. Mater.*, **2011**, *23*, 1436-1441.
- (20) Tao, Y.; Wang, Q.; Yang, C.; Zhong, C.; Qin, J.; Ma, D. *Adv. Funct. Mater.*, **2010**, *20*, 2923-2929.
- (21) Tao, Y.; Yang, C.; Qin, J. *Chem. Soc. Rev.*, **2011**, *40*, 2943-2970.
- (22) Mishra, A.; Fischer, M.K.; Bauerle, P.; *Angew. Chem. Int. Ed.*, **2009**, *48*, 2474-2499.
- (23) Lee, K-M.; Wu, S-J.; Chen, C-Y.; Wu, C-G.; Ikegami, M.; Miyoshi, K.; Miyasaka, T.; Ho, K-C. *J. Mater. Chem.*, **2009**, *19*, 5009-5015.
- (24) Yeh, H.-C.; Yeh, S.-J.; Chen, C.-T. *Chem. Commun.* **2003**, 2632-2633.
- (25) Chen, C.-T. *Chem. Mater.* **2004**, *16*, 4389-4400.
- (26) Kim, D. U.; Paik, S. H.; Kim, S.-H.; Tsutsui, T. *Synth. Met.* **2001**, *123*, 43-46.

- (27) Chen, H. Y.; Lam, J. W. Y.; Luo, J. D.; Ho, Y. L.; Tang, B. Z.; Zhu, D. B.; Wong, M.; Kwok, H. S. *Appl. Phys. Lett.* **2002**, *81*, 574-576.
- (28) Yamaguchi, Y.; Matsubara, Y.; Ochi, T.; Wakamiya, T.; Yoshida, Z. *J. Am. Chem. Soc.* **2008**, *130*, 13867.
- (29) Palayangoda, S. S.; Cai, X.; Adhikari, R. M.; Neckers, D. C. *Org. Lett.*, **2008**, *10*, 281.
- (30) Panthi, K.; Adhikari, R.M.; Kinstle, T.H. *J. Phys. Chem. A* **2010**, *114*, 4542-4549.
- (31) Palayangoda, S.S.; Cai, X.; Adhikari, R.M.; Neckers, D.C. *Org. Lett.*, **2008**, *10*, 2.
- (32) Zhang, W.; He, Z.; M, L.; Zou, Y.; Wang, Y.; Zhao, S. *Dyes and Pigments*, **2010**, *85*, 86-92.
- (33) Shen, X.Y.; Yuan, W.Z.; Liu, Y.; Zhao, Q.; Lu, P.; Ma, Y.; Williams, I.D.; Qin, A.; Sun, J.Z.; Tang, B.Z. *J. Phys. Chem. C* **2012**, *116*, 10541-10547.
- (34) Yang, Y.; An, F.; Liu, Z.; Zhang, X.; Zhou, M.; Li, W.; Hao, X.; Lee, C.-S.; Zhang, X. *Biomaterials*, **2012**, *33*, 7803-7809.
- (35) M Jr, B.; Moronne M.; Gin P.; Weiss S.; Alivisatos, A.P. *Semiconductor nanocrystals as fluorescent biological labels. Science* **1998**, *281*:2013-6.
- (36) Shen, X.Y.; Wang, Y.J.; Zhao, E.; Yuan, W.Z.; Liu, Y.; Lu, P.; Qin, A.; Ma, Y.; Sun, J.Z.; Tang, B.Z. *J. Phys. Chem. C* **2013**, *117*, 7334-7347.
- (37) Shen, M.; Rodriguez-Lopez, J.; Lee, Y-T.; Chen, C-T.; Fan, F-R. F.; Bard, A.J. *J. Phys. Chem. C* **2010**, *114*, 9772-9780.

- (38) Zhang, W.; He Z.; Pang, Y.W.H.; Zhao, S. *Thin Solid Films* **2012**, *520*, 2794-2799.
- (39) Kim, B-S.; Jindo, T.; Eto, R.; Shinohara, Y.; Son, Y-A.; Kim, S-H.; Matsumoto, S. *Crys. Eng. Comm.*, **2011**, *13*, 5374-5383.
- (40) Upamali, K.A.N.; Estrada, L.A.; De, P.K.; Cai, X.; Krause, J.A.; Neckers, D.C. *Langmuir* **2011**, *27*(5), 1573-1580.
- (41) Lai, R.Y.; Kong, X.; Jenekhe, S.A.; Brad, A.J. *J. Am. Chem. Soc.* **2003**, *125*, 12631-12639.
- (42) Qiu, X.P.; Lu, R.; Zhou, H.P.; Zhang, X.F.; Xu, T.H.; Liu, X.L.; Zhao, Y.Y. *Tetrahedron Lett.*, **2008**, *49*, 7446-7449.
- (43) Duesing, R.; Tapolsky, G.; Meyer, T.J. *J. Am. Chem. Soc.* **1990**, *112*, 5378-5379.
- (44) Jones Jr, W.E.; Chen, P.; Meyer, T.J. *J. Am. Chem. Soc.* **1992**, *114*, 387-388.
- (45) Spreitzer, H.; Daub, J. *Chem. Eur. J.* **1996**, *2*, 1150-1158.
- (46) Kramer, C.S.; Muller, T.J.J. *Eur. J. Org. Chem.* **2003**, 3534-3548.
- (47) Lai, R.Y.; Fabrizio, E.F.; Lu, L.; Jenekhe, S.A.; Brad, A.J. *J. Am. Chem. Soc.* **2001**, *123*, 9112-9118.
- (48) Zhang, X.-H.; Choi, S.-H.; Choi, D.H.; Ahn, K.-H. *Tetrahedron Lett.* **2005**, *46*, 5373-5276.
- (49) Meyer, T.; Ogermann, D.; Pankrath, A.; Kleinermanns, K.; Muller, T.J.J. *J. Org. Chem.*, **2012**, *77*, 3704-3715.

- (50) Cao, D.; Peng, J.; Hong, Y.; Fang, X.; Wang, L.; meier, H.; *Org. Lett.* **2011**, *13*, 1610-1613.
- (51) Xie, Z.; Midya, A.; Loh, K.P.; Adams, S.; Blackwood, D.J.; Wang, J.; Zhang, X.; Chen, Z. *Pro. Photovolt.Res. Appl.* **2010**, *18*, 573-58.
- (52) Kikuchi, D.; Sakaguchi, S.; Ishii, Y. *J. Org. Chem.* **1998**, *63*, 6023-6026
- (53) PCT. Int. Appl., 2008020203, 21 Feb **2008**
- (54) Yeh, H.-C.; Wu, W.-C.; Wen, Y.-S.; Dai, D.-C.; Wang, J.-K.; Chen, C.-T. *J. Org. Chem.* **2004**, *69*, 6455-6462.
- (55) Zhang, X.-H.; Kim, S.H.; Lee, I.S.; Goa, C.J.; Yang, S.I.; Ahn, K.-H. *Bull.Korean. Chem. Soc.* **2007**, *28*, 1389.



# Supporting Information

## Table of Contents

Figure Caption	Page No.
Figure S1. $^1\text{H}$ NMR spectrum of JK-1-08 recorded in $\text{CDCl}_3$	50
Figure S2. $^{13}\text{C}$ NMR spectrum of JK-1-08 recorded in DMSO	51
Figure S3. $^1\text{H}$ NMR spectrum of JK-1-12 recorded in $\text{CDCl}_3$	52
Figure S4. $^{13}\text{C}$ NMR spectrum of JK-1-12 recorded in $\text{CDCl}_3$	53
Figure S5. $^1\text{H}$ NMR spectrum of JK-1-20 recorded in $\text{CDCl}_3$	54
Figure S6. TGA-DTA-DTG plot of JK-1-08	55
Figure S7. TGA-DTA-DTG plot of JK-1-12	56
Figure S8. TGA-DTA-DTG plot of JK-1-20	57
Figure S9. IR spectrum of JK-1-08	58
Figure S10. IR spectrum of JK-1-12	59
Figure S11. IR spectrum of JK-1-20	60

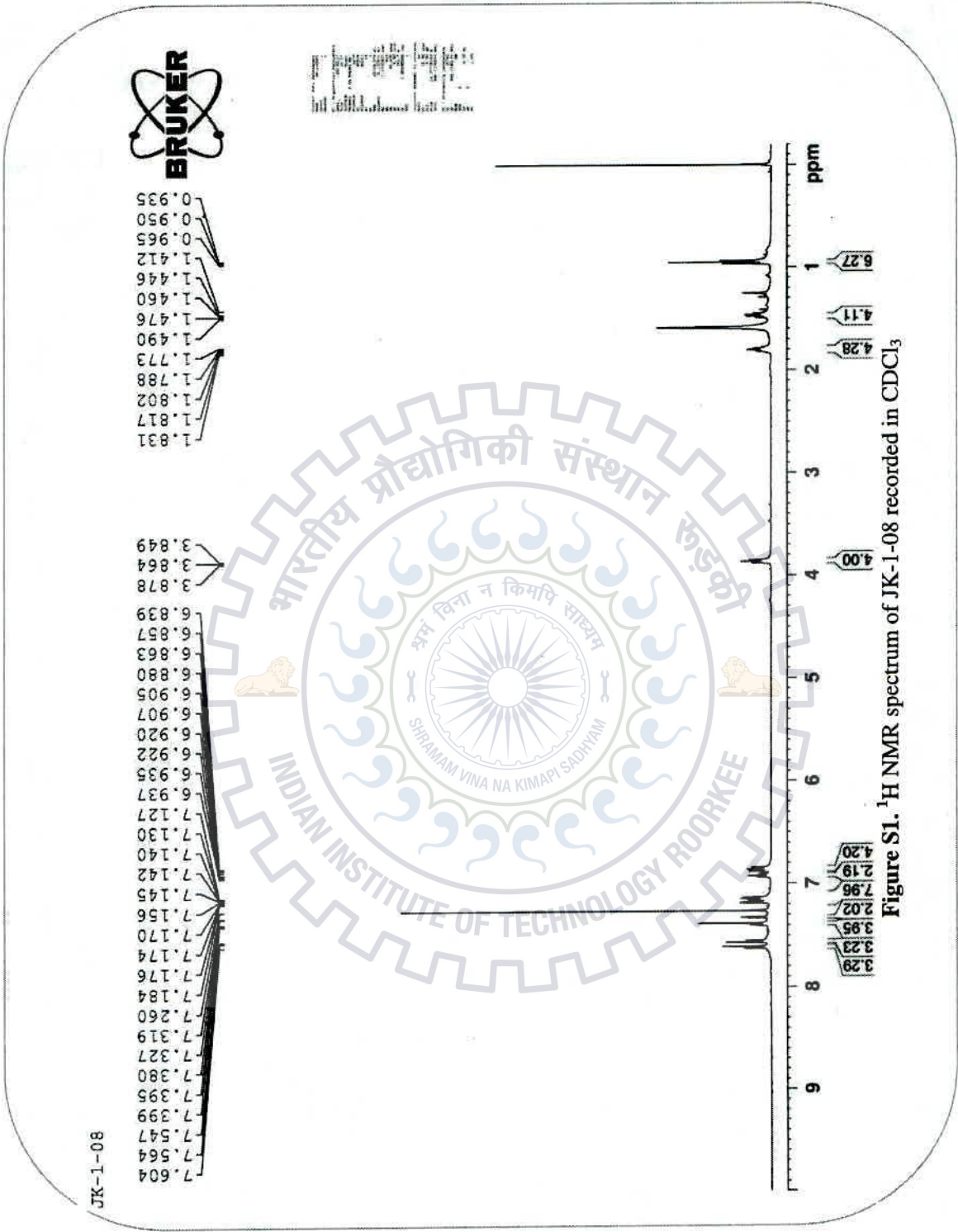


Figure S1. <sup>1</sup>H NMR spectrum of JK-1-08 recorded in CDCl<sub>3</sub>

JK-1-8 C13

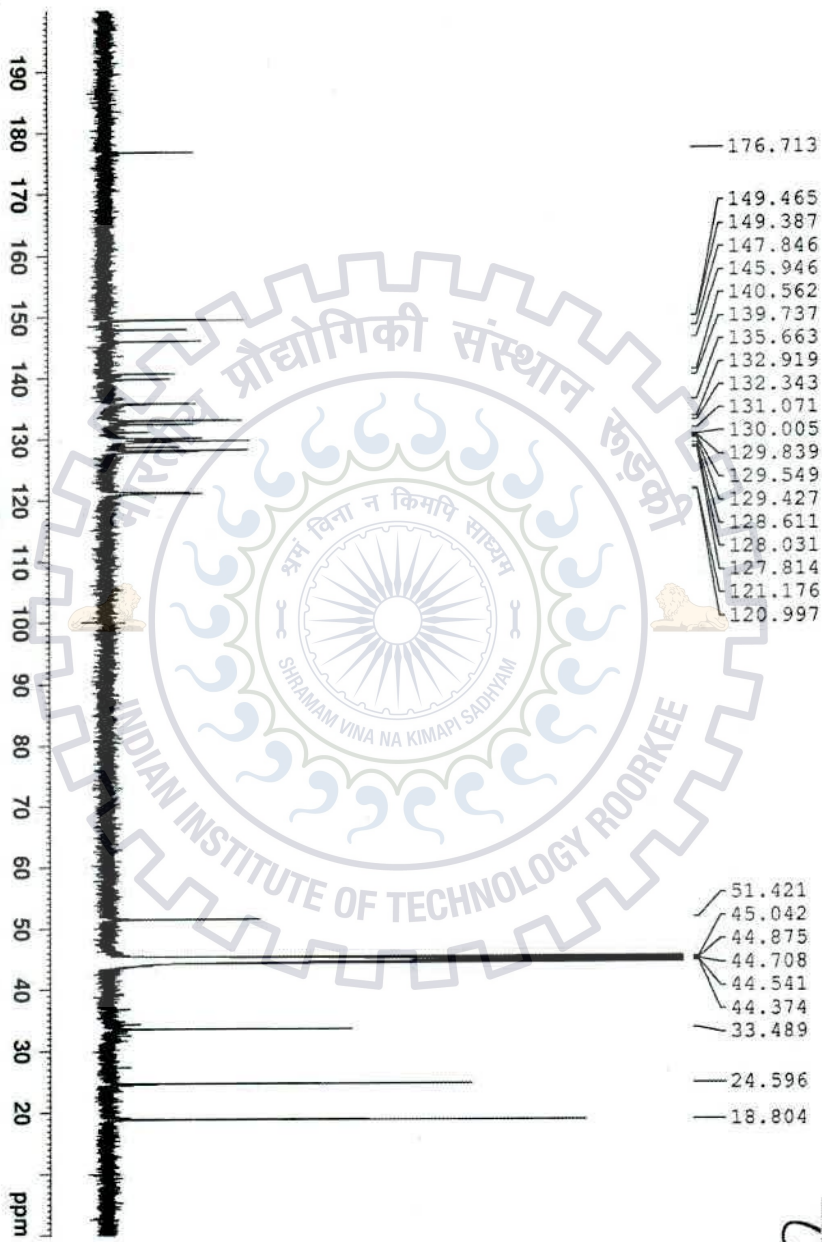


Figure S2.  $^{13}\text{C}$  NMR spectrum of JK-1-08 recorded in DMSO



INDIAN INSTITUTE OF TECHNOLOGY ROORKEE  
श्रम विना न किमपि साध्यम्  
SHRAMAM VINA NA KIMAPI SADHYAM





JK--1-12P F2

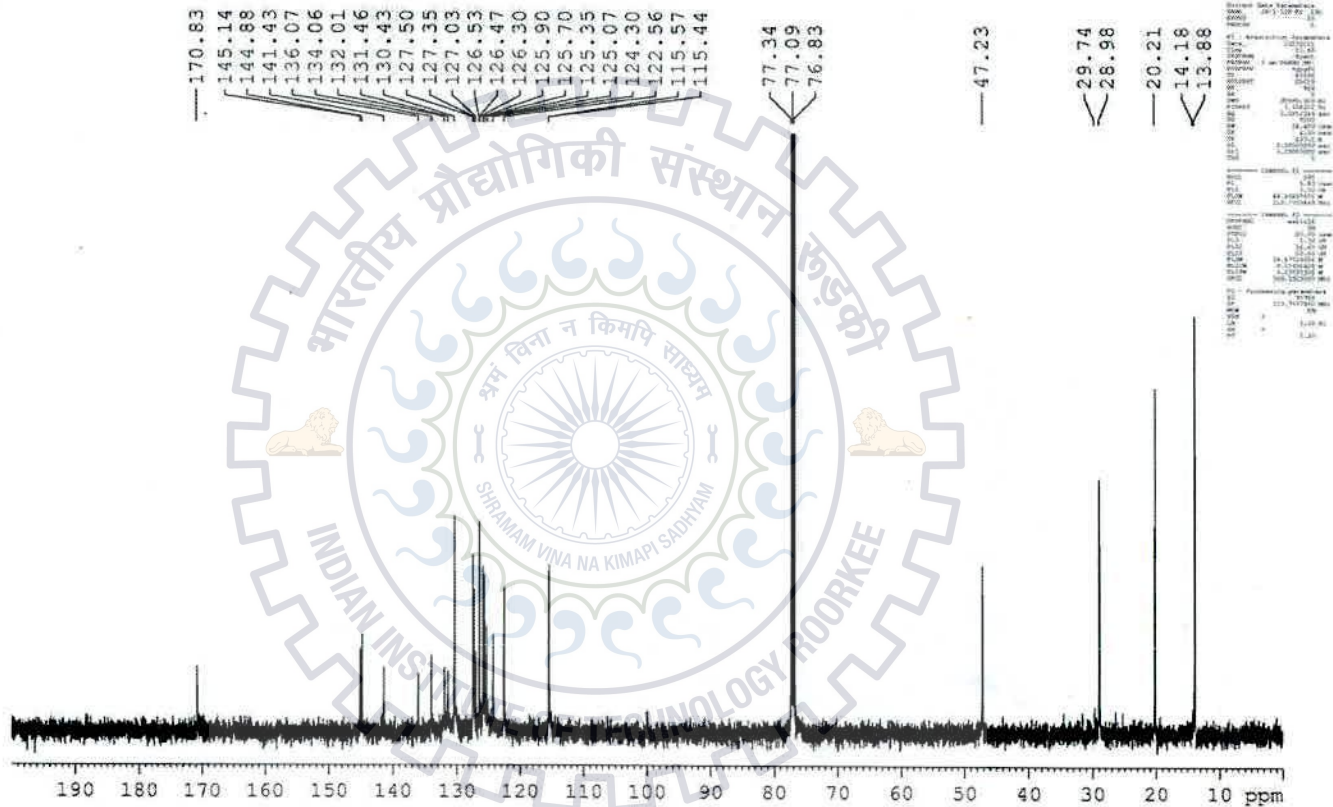


Figure S4.  $^{13}\text{C}$  NMR spectrum of JK-1-12 recorded in  $\text{CDCl}_3$

JK-1-20 A

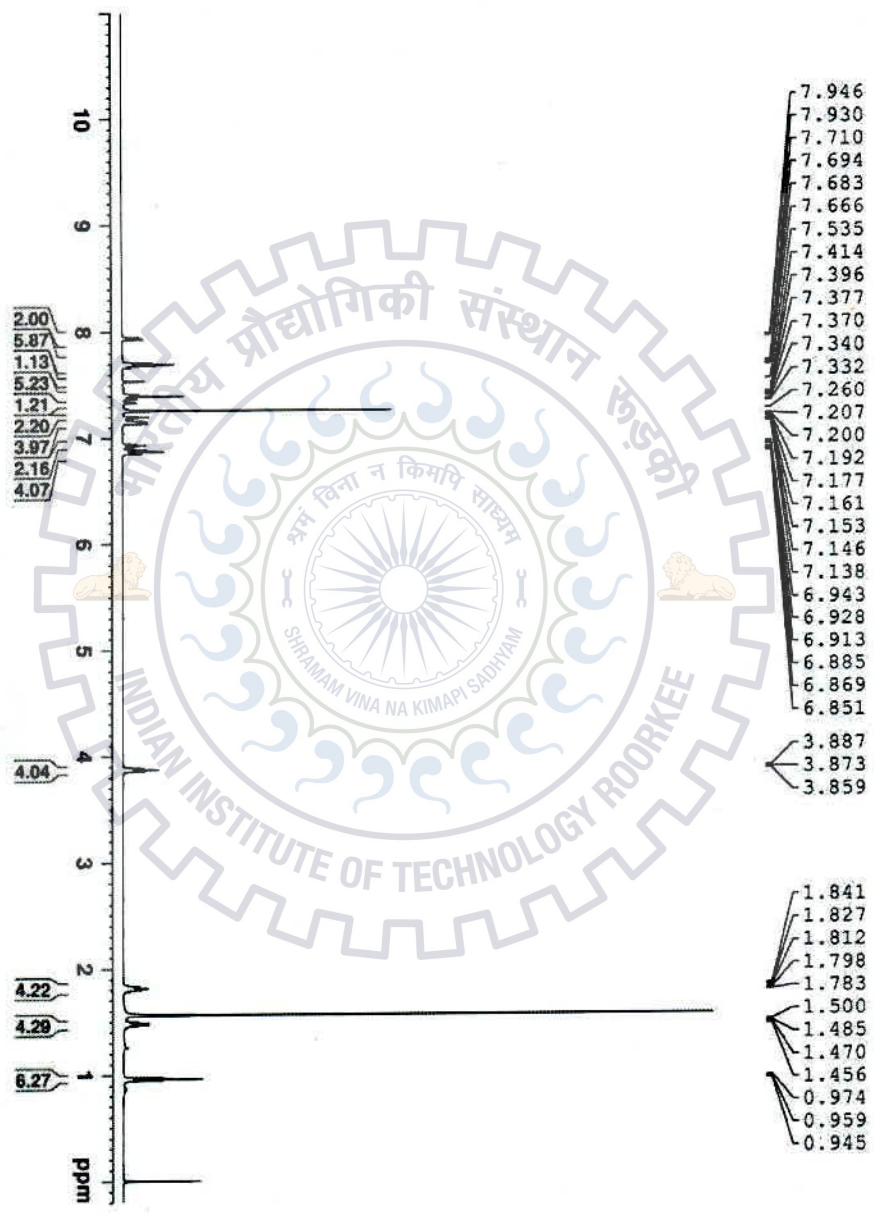


Figure S5. <sup>1</sup>H NMR spectrum of JK-1-20 recorded in CDCl<sub>3</sub>

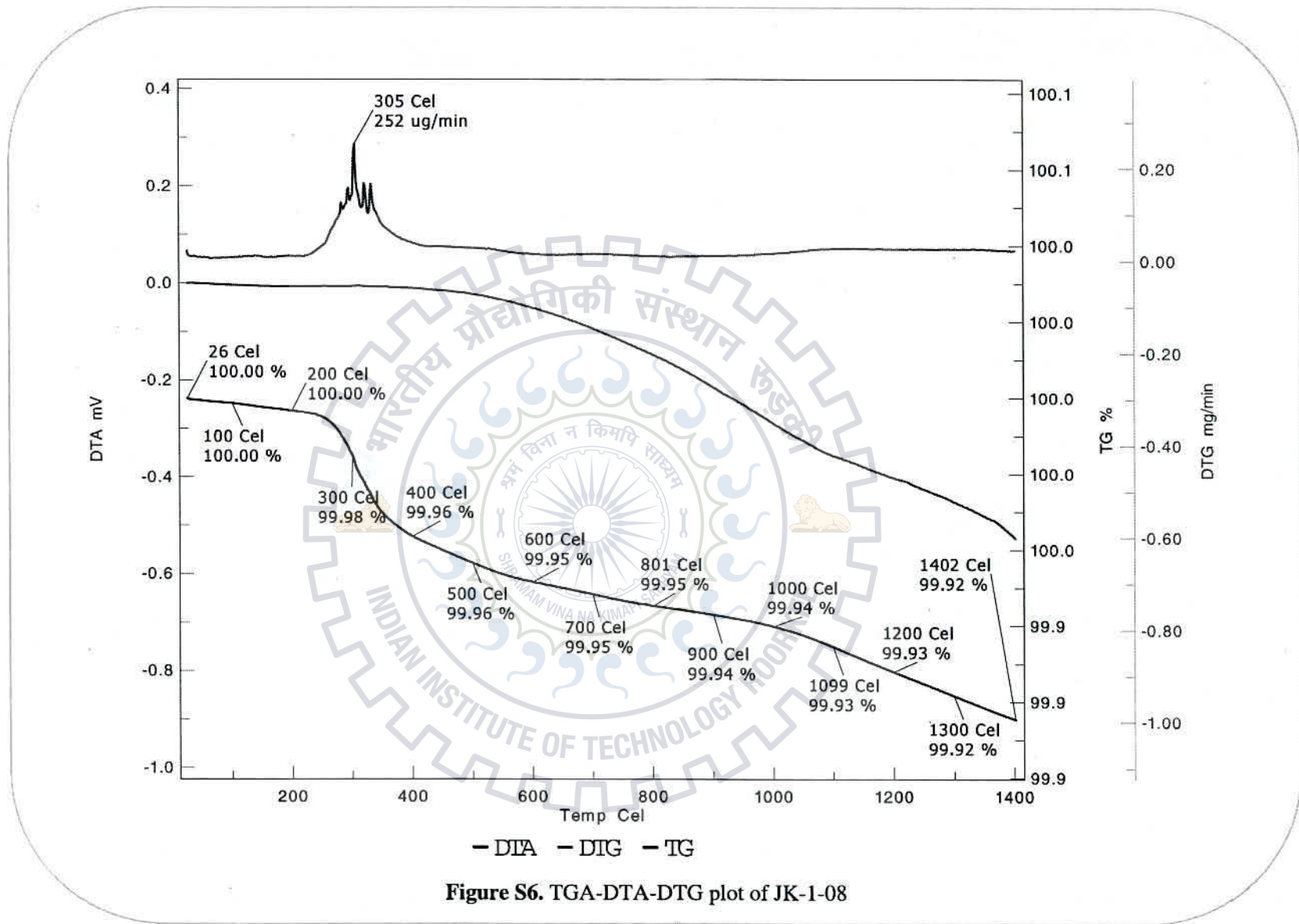


Figure S6. TGA-DTA-DTG plot of JK-1-08

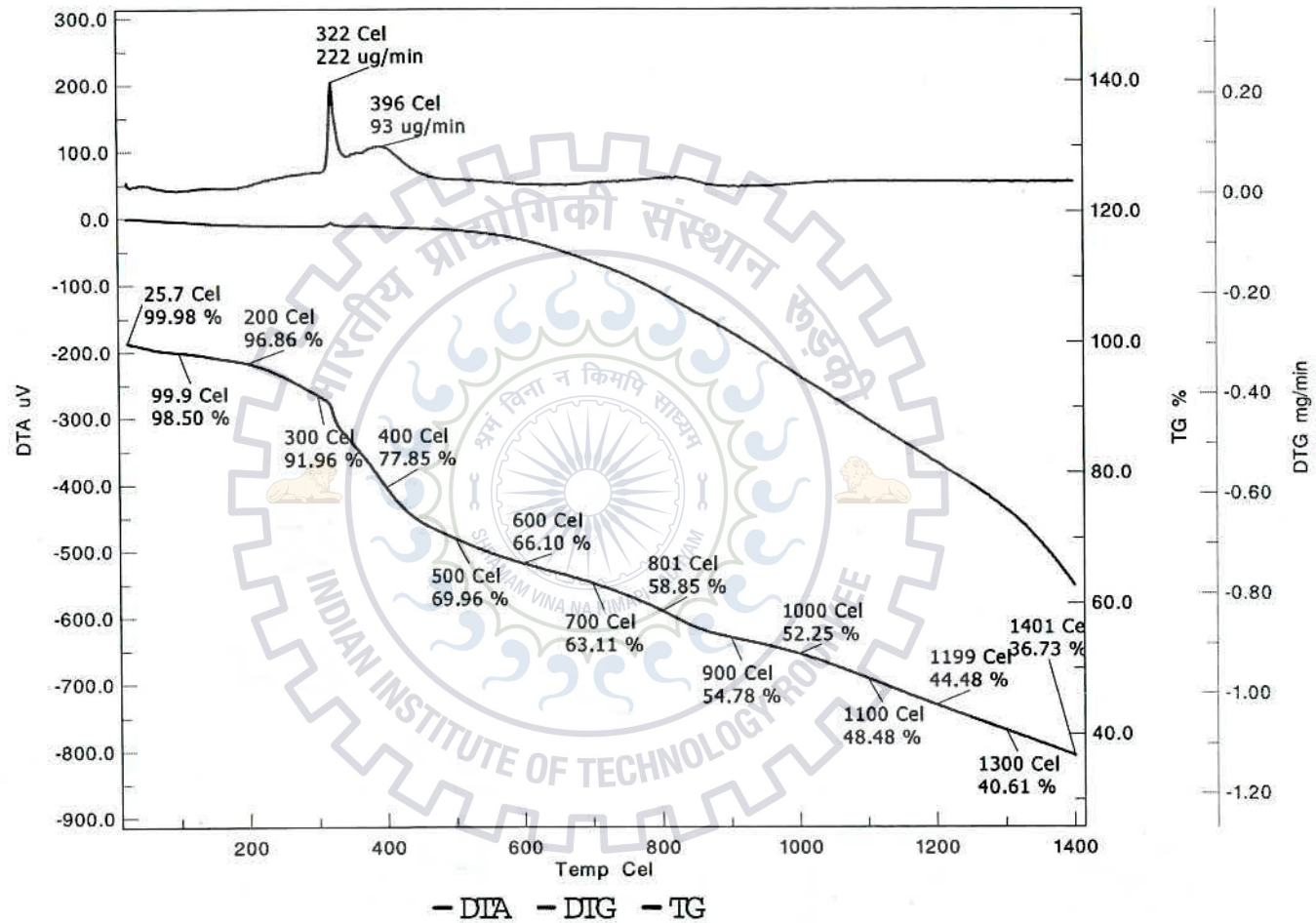


Figure S7. TGA-DTA-DTG plot of JK-1-12

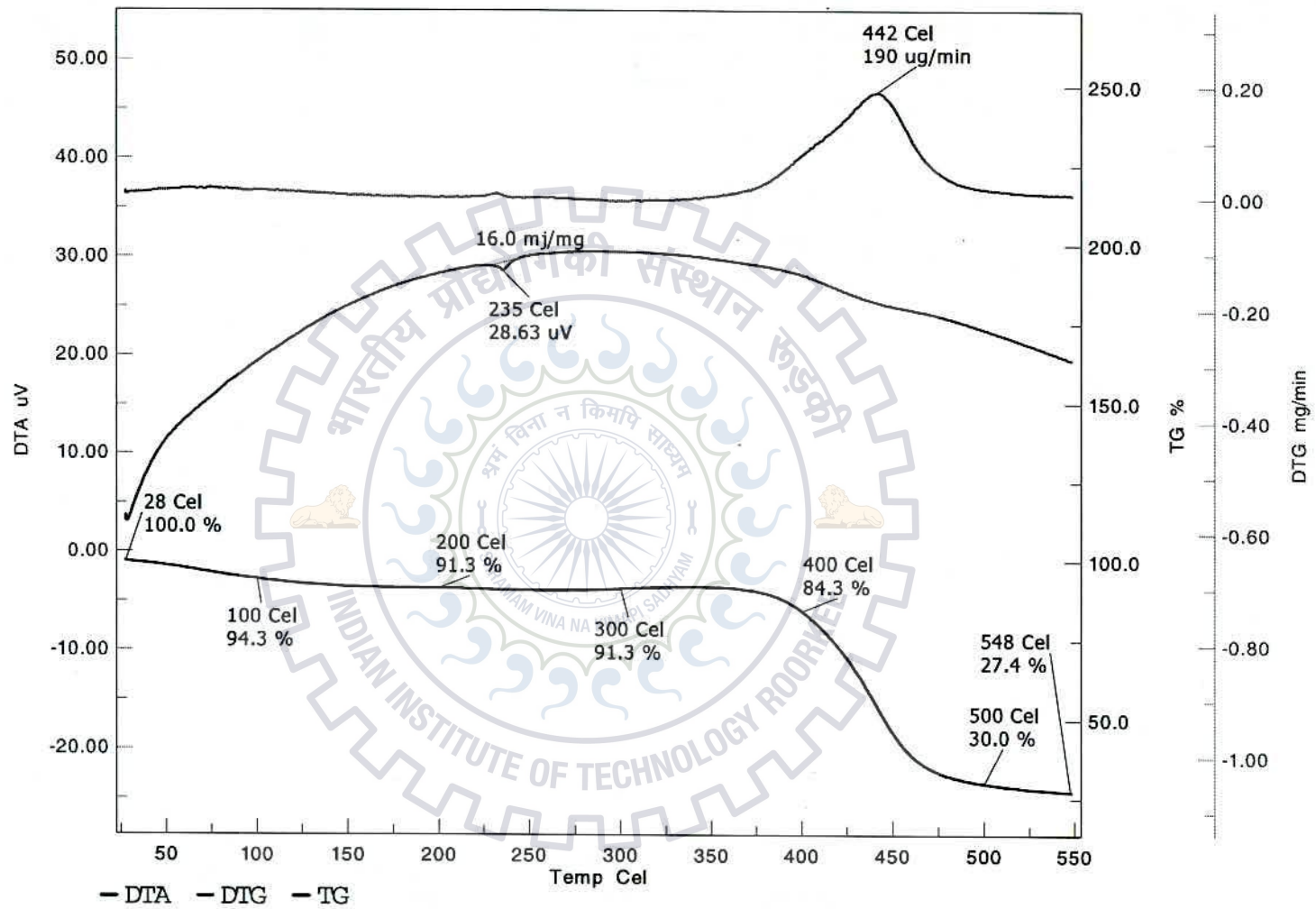


Figure S8. TGA-DTA-DTG plot of JK-1-20

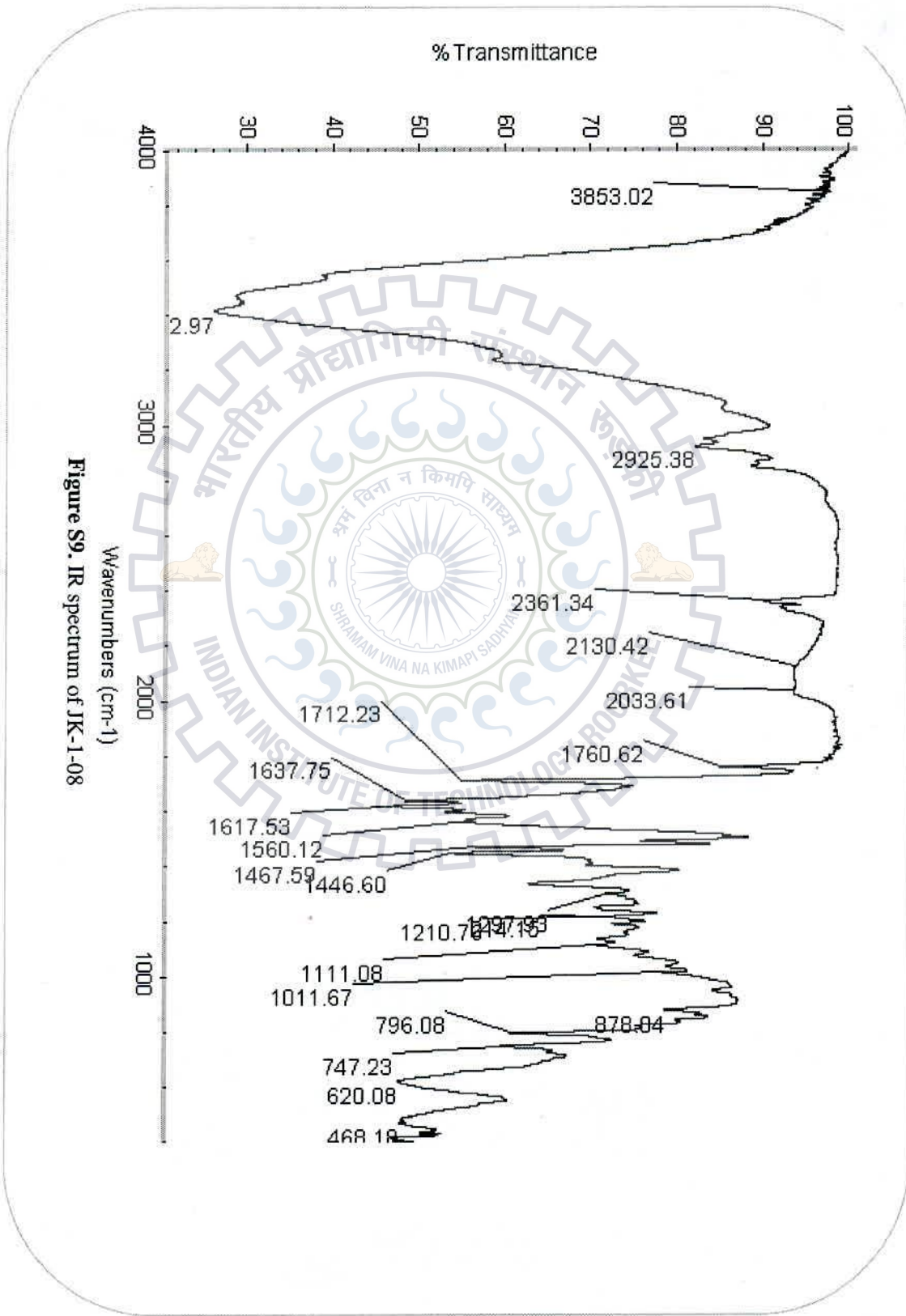


Figure S9. IR spectrum of JK-1-08

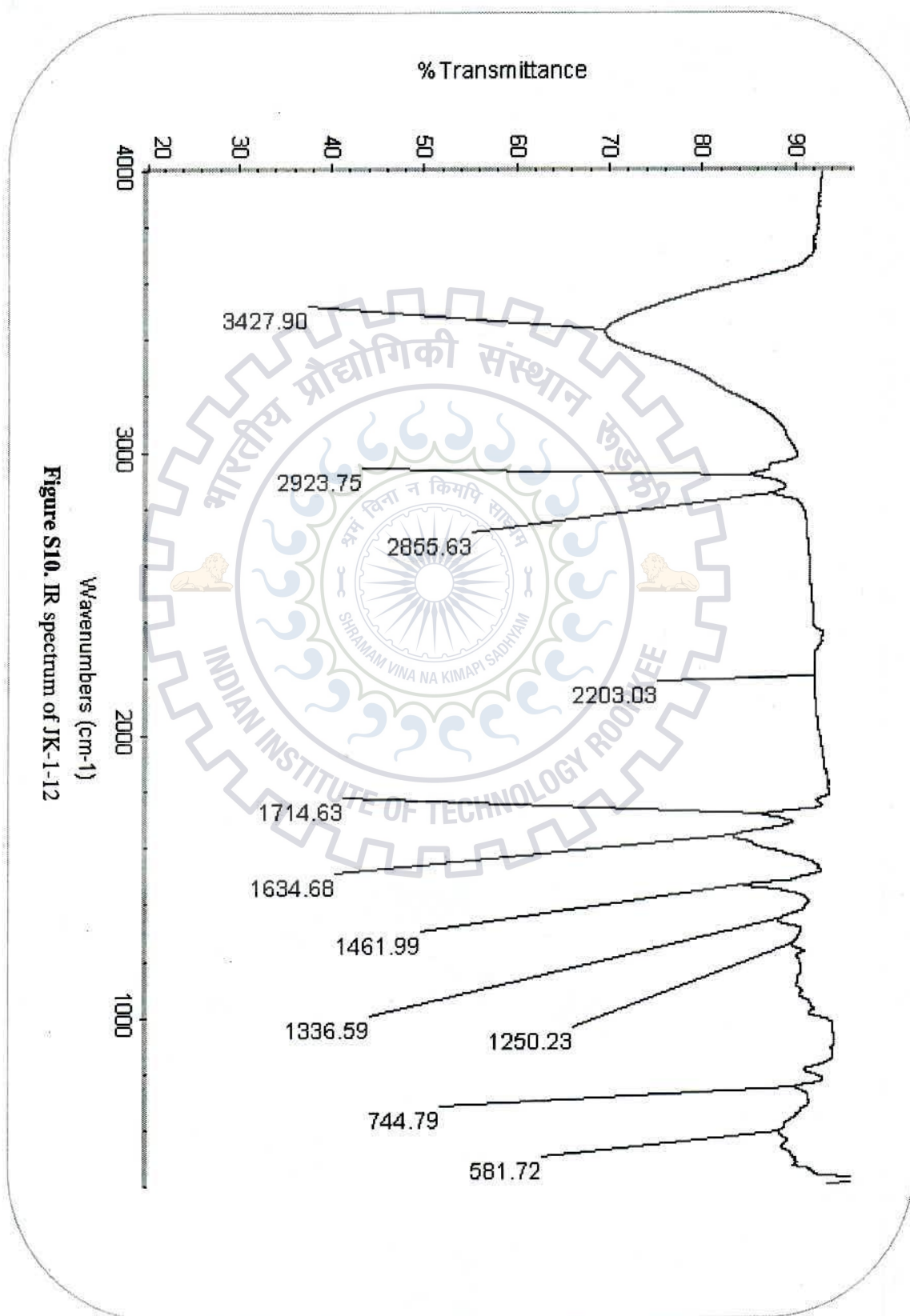


Figure S10. IR spectrum of JK-1-12

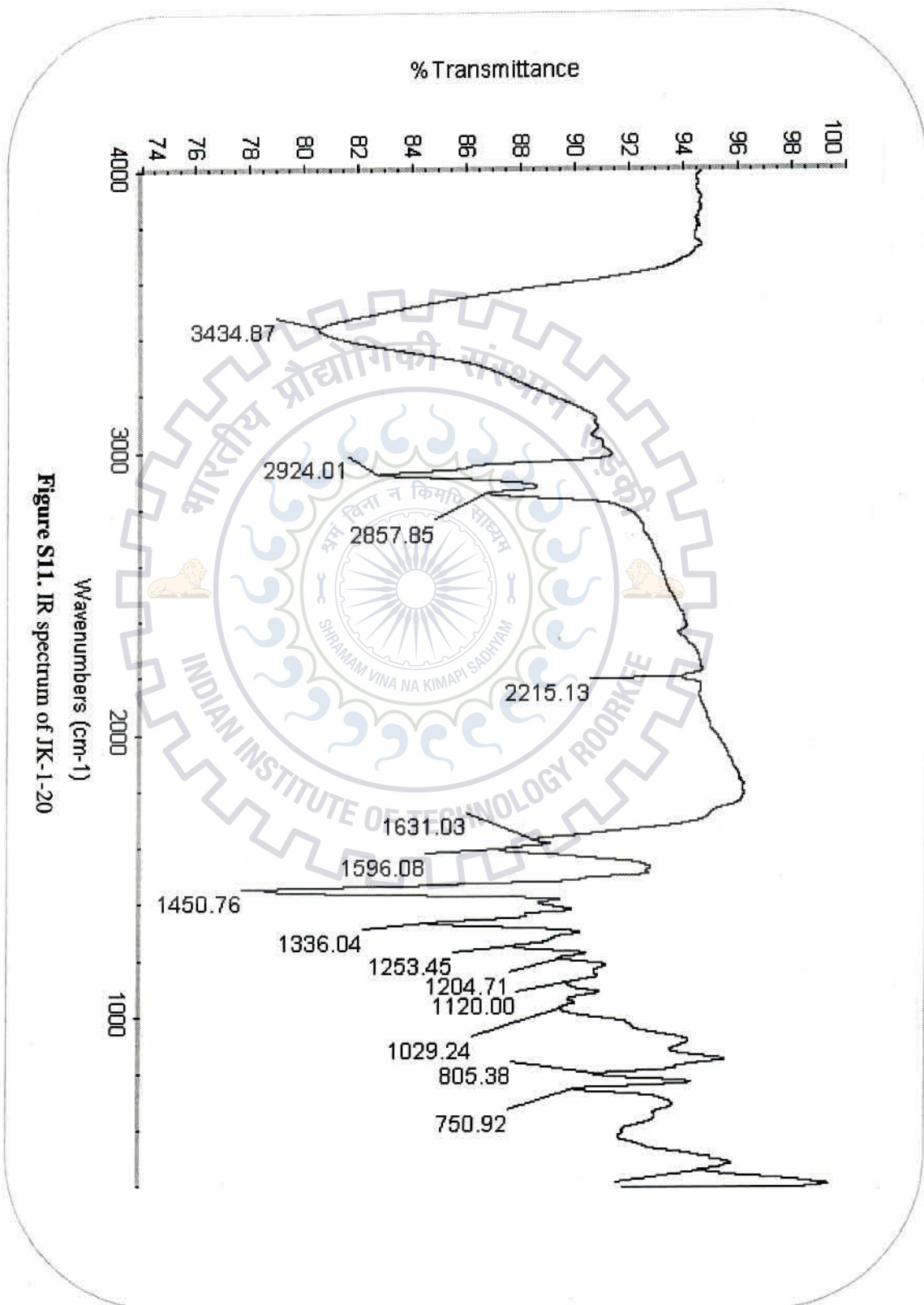


Figure S11. IR spectrum of JK-1-20